2021

Identification of Compounds Causing Cellular Autofluorescence in Touch Samples

Elora C. Wall
Virginia Commonwealth University

Identification of Compounds Causing Cellular Autofluorescence in Touch Samples

Elora Wall

Ehrhardt Laboratory

Partial fulfillment statement:

A thesis submitted in partial fulfillment of the requirements for the degree of Master of Science in Forensic Science at Virginia Commonwealth University.

Acknowledgements

First and foremost, I would like to thank Dr. Christopher Ehrhardt for guiding me through this project, as well as Dr. Joseph Turner for training and assisting me with the instrumentation and Eric Hazelrigg for serving on my Directed Research Committee. I would also like to thank Sarah Ingram for her support, both technically and emotionally, throughout this project. Finally, I would like to thank my family, specifically my husband, parents, and in-laws, and friends for their love and continued support.

Abstract

As DNA analysis has advanced and produced tests with higher sensitivities, attention has turned toward obtaining DNA profiles from cells left with fingermarks. Recent studies have reported that cells deposited within fingermarks can exhibit differences in autofluorescence emission in the 'red' region of the visible spectrum (e.g., between 650-670 nm), which can be used to differentiate contributor cell population and separate them before DNA profiles. Interestingly, this emission was not consistent to the individual day-to-day and likely not a genetically-controlled attribute of the contributor. Instead, this emission signature results from extended exposure of the skin to certain materials such as plant material (e.g. kale, collard greens), purple nitrile gloves, and some marker ink (e.g. black or green ink) (Katherine Philpott, 2017). As of yet, the molecule(s) causing this unique signature has not been identified. The purpose of this project is to develop a pathway for elucidating the identity of compounds with specific fluorescent signatures present in fingermarks. This project focuses on the identification of the compound(s) deposited by kale which is responsible for the autofluorescence signature seen between 650 nm and 670 nm.

To accomplish this, the compound(s) of interest was first extracted from kale leaves using isopropyl alcohol. The extracted compound(s) were then analyzed using fluorescence spectroscopy, Fourier Transform Infrared Spectroscopy (FTIR), Direct Analysis in Real Time Mass Spectrometry (DART-MS), High Performance Liquid Chromatography (HPLC), and Gas Chromatography-Mass Spectrometry (GC-MS). Touch samples were collected after handling kale, and the resulting samples were also analyzed using fluorescence spectroscopy, flow cytometry, and DART-MS.

Both the kale extract and kale touch samples exhibited excitation peaks at 435 nm and emission peaks at 665 nm when analyzed with fluorescence spectroscopy, which is consistent with the previous study. When the extract was analyzed using FTIR, the signature seen was similar to that of beeswax indicating that the fluorescent compound may be inherent to the kale. To determine this, extracts and touch samples were obtained from both store-bought kale and home-grown kale and fluorescent signatures from both were consistent, indicating that the compound(s) of interest are inherent to the kale. When the touch samples, extract, and kale leaves were analyzed with DART-MS, a common peak of 423.45 m/z was seen in all three. HPLC was performed on the extract in an attempt to isolate the compound for mass spectrometry analysis but was unsuccessful. GC-MS was also performed on the extract, but the 423 m/z was not seen.

Some glucosinolates were considered as possible identities for the target compound but were eliminated due to differences in both fluorescence and DART-MS with standards of gluconasturtiin and glucoiberin. Currently, LC-MS is being explored to isolate the compound and attempt to gain more fragmentation information about the compound. Ultimately, the scheme used for this compound identification will provide a foundational mechanism that can be used to identify other fluorescent compounds seen with fingermarks.

Keywords: Fluorescence, fingermarks, DART-MS, touch samples, FTIR, flow cytometry

Introduction

As DNA analysis has advanced and produced tests with higher sensitivities, attention has turned toward obtaining DNA profiles from biological samples deposited with fingermarks. These DNA samples are commonly referred to as 'touch' or trace samples, as the DNA and/or biological material are often deposited in trace amounts as an individual touches a surface. If multiple people touch a single surface, the sample can contain DNA from multiple contributors. This presents a problem for determining individual DNA profiles from the mixture, as it can be difficult to attribute individual alleles to each contributor or even to determine the number of contributors present. (Executive Office of the President President's Council of Advisors on Science and Technology, 2016) (van Oorschot, 2010)

One potential solution is to perform front-end separation of cells from different contributors before performing DNA analyses. While there have been some techniques explored for separating cells, it can be difficult to differentiate cells of the same type from different contributors without the use of some type of tag (e.g. antibody probe). Even so, this can be problematic for epithelial cells in touch samples, as binding sites for these probes change throughout cell maturation and prior to cell shedding (Marek Haftek, 1986). Therefore, it is imperative to be able to distinguish between cells that are distinctive due to differences from the donors.

Recent studies have shown that cells deposited within fingermarks can exhibit differences in autofluorescence emission in the 'red' region of the visible spectrum (e.g., between 650-670 nm), which can be used to differentiate contributor cell population and also separate them before DNA profiling (Philpott, 2017) (Stanciu, 2016). Interestingly, this emission was not consistent with the individual day-to-day and likely not a genetically controlled attribute of the contributor

(Stanciu, 2016). Instead, this emission signature results from extended exposure of the skin to certain materials such as plant material (e.g. kale, collard greens), purple nitrile gloves, and some marker ink (e.g. black or green ink) (Philpott, 2017).

While this is a promising tool for differentiating and ultimately separating contributor cell populations, the molecule(s) responsible for the autofluorescent signature has not been identified. This identification could be useful not only for cell separation but also applications involving individual tracking. These autofluorescent compounds likely have strong lipophilic characteristics, as they not only adhere to epidermal cell layers but also can persist after hand washing.

Therefore, the goal of this project was to determine the identity of the target compound(s). To accomplish this, an interdisciplinary approach was used to isolate the compound of interest, then identify it using orthogonal analytical strategies. First, the target compound was extracted and analyzed using Fourier Transform Infrared Spectroscopy (FTIR) and Direct Analysis in Real Time-Mass Spectrometry (DART-MS). Next, the transfer experiments from the previous study (Philpott, 2017) were repeated and the cells were analyzed using DART-MS to confirm that the target molecule was present in the extract. Then the target molecule was isolated and analyzed using HPLC-FLD coupled with DART-MS, Gas Chromatography-Mass Spectrometry (GC-MS), and Liquid Chromatography-Tandem Mass Spectrometry (LC-MS/MS).

Materials and Methods

Solubility Test

To determine the best solvent to extract the target compound and observe its autofluorescence, approximately 0.5 g of kale was placed in the top of a glass culture tube (Fisherbrand, 16x125 mm, Cat. No. 14-961-30) that had been rinsed with hexanes (EM Science, Lot 42205), toluene (Fisher Chemicals, Lot 031222), isopropanol (Pharmco-AAPER, Lot K16C03026), methanol (EMD, Lot 54276), or acetonitrile (Fisher Scientific, 130339). Each sample was then rinsed with 5 mL each of the corresponding solvent. The resulting solution was then analyzed using fluorescence spectroscopy to determine autofluorescence excitation/emission profiles. The isopropanol solution showed the highest intensity fluorescence at a wavelength of ~670 nm with excitation at ~ 430 nm followed closely by methanol. Isopropanol was therefore chosen for extraction of the compound for further analysis and methanol was used when isopropanol was not appropriate.

Extraction

Extraction methods were tested by placing approximately 0.5 g of kale in each glass culture tube which was then either rinsed with 5 mL isopropanol, soaked in 5 mL isopropanol for 15 min or vortexed in 5 mL isopropanol for 30 s. The fluorescence of each of the resulting solutions was then measured. Soaking the kale in isopropanol resulted in higher fluorescence than the other techniques indicating that was a more effective extraction method. Therefore, it was adopted for some DART-MS and HPLC experiments as well as all GC-FID, GC-MS, and LC-MS/MS experiments.

Collection of touch samples

To confirm that handling kale would result in a shift in fluorescence in touch samples, touch sample experiments performed in the previous study were repeated (Katherine Philpott, 2017). Touch samples were obtained following procedures of the previous study and in accordance with the VCU-IRB protocol #HM20000454_CR7. Volunteers first washed their hands for approximately 20 seconds and allowed their hands to air dry. They then handled a piece of kale in one hand for 5 min, the other hand did not come into contact with any kale which was not used to served as a control. Hands were then rinsed to remove any visible kale residue from their hands and allowed to air dry. They then handled a conical tube in each hand for 5 min. Each tube was then swabbed with a cotton swab wetted in 2 mL of deionized water and then with a dry swab. Both swabs were placed in the deionized water and vortexed for 90 s. Samples were then centrifuged at 14,549 g for 10 min and the resulting supernatant was removed. The cell pellet was then resuspended in 500 µL cell staining buffer (BioLegend, Lot B235811) and vortexed. The resulting suspension was filtered by passing through a 100 µm filter mesh and analyzed using flow cytometry.

Fluorescence

Fluorescence analysis was performed on the Varian Cary Eclipse Fluorescence Spectrophotometer. Analysis was performed in both excitation and emission mode with excitation wavelengths of 430-435 nm and emission wavelengths of 660-680 nm and a slit width of 5 nm for both the excitation and emission slit. Data were collected with a scan rate of 1200.00 nm/min, a data interval of 2.0 m, and an average time of 0.1000 s.

FTIR

Fourier Transform Infrared Spectroscopy analysis was performed on the Nicolet iS50 FT-IR with a DTGS detector and an iS50 ATR module with a KBr beamsplitter and an optical velocity of 0.4747. A drop of the kale extract solution was deposited on the ATR crystal. The isopropanol was allowed to evaporate and then a scan was obtained. A control was performed using isopropanol from the same source as was used to make the extract to confirm that it was completely evaporated and not affecting the FT-IR spectrum of the target compound. The HR Comprehensive Forensic FT-IR Collection library was used to search for compounds with similar spectra.

Flow Cytometry Flow cytometry analysis of eluted cells was performed on a Millipore Guava EasyCyte 5 (MilliporeSigma, Burlington, MA) equipped with a 488 nm laser and 3 detector channels of Green-B (525/30 nm), Yellow-B (538/26 nm), and Red-B (695/50 nm). Analysis of fluorescence data was performed using the FlowJo software.

Imaging Flow Cytometry

Imaging flow cytometry of eluted cells was performed on the AMNIS ImageStream X Mark II (Luminex, Austin, TX) equipped with 488 nm and 642 nm lasers. Individual event images were captured in the brightfield and allophycocyanin (APC) (642-745 nm) channels. Cell images were analyzed using the IDEAS® Software (EMD Millipore).

DART-MS

Mass Spectrometry was performed using an IonSense Direct Analysis in Real Time ion source with a AccuTOF mass spectrometer (JEOL, Peabody, MA). Analyses in positive mode were performed with helium carrier gas, an oven temperature of 350º C, and with an orifice voltage of 20V, 30V, 60V, 80V, 90V, and 120V. Analyses in negative mode were performed with helium

carrier gas, an oven temperature of 350º C, and with an orifice voltage of 20V. Library searches were performed in the NIST library.

HPLC

High Performance Liquid Chromatography was performed using an Agilent Technologies 1260 Infinity HPLC. A Waters µBondapak C18 125Å 10 µm 150mm column (Lot# W33251) was used with a mobile phase of 30% Acetonitrile 70% water. A fluorescence detector was used with an excitation wavelength of 435 nm as well as a diode array detector with absorbance wavelengths of 435 nm and 633 nm.

GC-MS

Gas Chromatography-Mass Spectrometry of the kale extract was performed using an Agilent 6890 GC with an Agilent DB-1MS column. An initial oven temperature of 50ºC was used with a final temperature ranging 260ºC-320ºC with a ramp time ranging 15ºC/min-30ºC/min and an initial hold time off 2 min. An inlet temperature of 250ºC was used for both splitless and split (10:1 and 20:1).

Gas Chromatography-Mass Spectrometry of the kale extract was performed on a Shimadzu GC-MS with a Restek RXI-5MS column. An initial oven temperature of 50ºC was used with a final temperature of 260ºC with an initial hold of 2 min with a ramp time of 15 ºC/min with a final hold of 20 min.

A 1:10 dilution of the kale extract was performed on a Shimadzu Gas Chromatograph GC-2010 Plus with a GCMS-QP2020 Gas Chromatograph Mass Spectrometer with an Agilent HP-5MS column. An initial oven temperature of 70ºC was used with a final temperature of 300ºC with an initial hold of 1 min with a ramp rate of 15 ºC/min and a final hold of 20 min.

LC-MS/MS

Liquid Chromatography with tandem Mass Spectrometry was performed on a Shimadzu LCMS-8050 Liquid Chromatograph Mass Spectrometer with an Agilent Infinity Lab Poroshell 120 EC-C18 2.1x50 mm 2.7- µm column. The mobile phase was a mixture of Solvent A (998 mL water, 0.315 g ammonium formate, 1 mL formic acid) and Solvent B (acetonitrile) gradient from 100% Solvent A/0% Solvent B to 20% Solvent A/80% Solvent B over 7 min with a flow rate of 0.5 mL/min. Detection was performed with a total ion scan with fragmentation.

Results and Discussion

FTIR

Once the solvent for extraction was determined, FTIR was performed to characterize the structure of the target compound. A broad peak centered at 3346.92 cm^{-1}, a strong, sharp peak at 2915.90 cm^{-1}, and two weaker, sharp peaks at 2969.09 cm^{-1} and 2848.40 cm^{-1} were seen in the functional group region of the IR spectrum while peaks at 1472.00 cm^{-1}, 1462.96 cm^{-1}, 1378.00 cm^{-1}, 1157.95 cm^{-1}, 1129.14 cm^{-1}, 951 cm^{-1}, 902.57 cm^{-1} and 719.33 cm^{-1} were seen in the fingerprint region of the IR spectrum (Figure 1). Peaks at 3346.92 cm^{-1}, 2915.90 cm^{-1}, 2969.09 cm^{-1}, and 2848.40 cm^{-1} indicate that there is a bonded OH, likely part of a carboxylic acid, in the compound while peaks at 951 cm^{-1}, 902.57 cm^{-1}, and 719.33 cm^{-1} indicate that a double bond between two carbons is likely present. When a library search was performed on the spectra, a 91.48% match was found with beeswax with other matches being other types of wax. This indicated that the compound could potentially be consistent with a wax compound intrinsic to the kale such as the epicuticular wax compounds found in kale leaves (Hama, 2019).

Homegrown vs. Commercial

To determine if the target compound was an intrinsic component of the wax-like compounds of the kale or an exogenous component (i.e., preservative), the fluorescence of extracts from homegrown kale and commercial kale were compared (Figure 2). The former type of kale was not treated with any pesticides. The fluorescence of the store-bought and homegrown kale was observed using excitation wavelengths of 432-434 nm and emission wavelengths of 665-670 nm. Similar excitation and emission were seen between the two samples, indicating that the target compound was a natural component of the kale and not an added compound.

Fluorescence of 'Touch' Epidermal Cell Samples

Samples were collected from volunteers after they handled kale with one hand, the other serving as a control, and were analyzed using both conventional flow cytometry and imaging flow cytometry. Though the intensity of the fluorescence of touch samples was approximately 35 a.u. lower than that of the kale extract for both emission and excitation, it is still evident that there is a noticeable emission peak at 680 nm when excited with 435nm (Figure 3). Flow cytometry results indicated a clear difference in the median autofluorescence of the major control cell peak around 10^3, and the median autofluorescence of the major peak for cells after handling kale around 10^4 (Figure 4). This indicates that cells collected after handling kale have a higher intensity of red autofluorescence compared to control cells. Additionally, touch cell samples were analyzed using imaging flow cytometry, where the fluorescence of cells after handling kale was more than double that of control samples from multiple donors (Figure 5). While it appears that the opposite of this trend was seen for donor D, DART-MS data suggests that these samples were mislabeled (discussed below). This indicates that there is a transfer of a fluorescent compound or compounds from the kale to the cells before depositing touch samples.

DART-MS

Touch samples consisting of shed epidermal cells and other biological material obtained after handling kale, kale extract in isopropanol, and a kale leaf were all analyzed using DART-MS to determine if there were any common mass peaks present in all three that could potentially be attributed to the target compound. Very few peaks were present in comparison to the kale extract and the kale leaf. However, all three samples had a peak at 423.4502 m/z +/- 0.0001 m/z (Figure 6). A library search of this compound yielded a match (38.8% total spectrum, 63.5% for masses above 350 m/z) to 22-desoxycarpesterol (546.8 g/mol, CAS ID 40129-53-1).

DART-MS was performed on the kale extract at several different voltages (20V, 30V, 60V, 90V, and 120V) to fragment the target compound at 423 m/z. However, the 423.4617 m/z +/- 0.0045 m/z persisted at 120V indicating that the compound is very stable and resistant to fragmentation (Figure 7).

DART-MS was also performed on the kale extract in negative mode suspecting that the compound may be similar in structure to a lipid and would therefore ionize and fragment more readily. When this was done at 20V, peaks were seen at 359.1273 m/z and 456.4556 m/z (Figure 8).

HPLC

Based on fluorescence and mass spectrometry data, it was unclear how pure the extracted target compound was. Therefore, HPLC was employed to assess purity and, subsequently, isolate the compound(s) of interest. Because the excitation and emission wavelengths of the compound were known, these were used for detection of the compound with a fluorescence detector set for excitation of 435nm and emission of 680nm. Diode array detectors at 435 nm and 633 nm were also used. When the compound was extracted with a mobile phase of 50% methanol 50% water using a C18 column, the peak was not detected. When the compound was extracted with isopropanol and run with a mobile phase of 30% acetonitrile 70% water, the target compound eluted around 6 min (Figure 9). Once the retention time of the target compound was identified, fraction collection was attempted to obtain the isolated compound from both kale extract and collard greens extract. Fractions were examined for fluorescence and by DART-MS to see if the target compound was present. The compound was not identified in any of the fractions with fluorescence and it was only found in one collard green fraction using DART-MS (Figure 10).

However, the presence of the target compound was confirmed before separation for each extract using DART-MS.

Comparison to Standards

Once the mass of the target compound was identified from DART-MS as 423.45 m/z +/- 0.01 m/z, a literature search was performed to find known compounds present in kale with this mass. Two glucosinolates, (1) gluconasturtiin (423.5 g/mol) and (2) glucoiberin (423.5 g/mol), were identified (Steglich, 2000) (Rahman, 2014) (Doheny-Adams, 2017). Gluconasturtiin and glucoiberin were obtained to compare with the target compound. Both compounds were put in isopropyl alcohol for direct comparison to the extracted target compound, however, neither compound appeared to be soluble. This may indicate that neither glucosinolates were the same compound as the unknown target compound. For both compounds, the isopropanol solution and the pure powder were analyzed using DART-MS in positive mode at multiple voltages (20V, 30V, 60V, 90V and 120V). The 423.45 m/z of the target compound was not seen in either gluconasturtiin (Figure 11) or glucoiberin (Figure 12). Additionally, the autofluorescence of gluconasturtiin was observed with an excitation wavelength of 435 nm and an emission wavelength of 670 nm (Figure 13). Gluconasturtiin did not exhibit an autofluorescence profile consistent with the target compound. Furthermore, both compounds exhibited more fragmentation with increasing voltage, with the molecular ion absent at 120V, whereas the target compound is still intact at 120V. This indicates that the structure of the target compound is more stable and less susceptible to fragmentation than that of both gluconasturtiin and glucoiberin. Therefore, it seems that the target compound is a member of the glucosinolate class.

GC-MS

Gas Chromatography-Mass Spectrometry analyses were initially performed on an Agilent GC-FID-MS with a DB-1ms column both with a 10:1 split and splitless injection. With the 20:1 split, some peaks were barely visible and the corresponding mass spectra did not show the target of mass of 423.45 m/z (Figure 14). When the sample was run with no split, peaks were not visible (Figure 15). Instead, an m/z of 207 was present, which could be an indication of column or septum bleed or could potentially indicate the presence of lipids (Agilent Technologies). Additionally, the extract was run again with an increased oven temperature and increased ramp rates, no discernible peaks were visible (Figure 16 and 17).

When the extract was analyzed using an RXI-5MS column, a distinct peak was observed at a retention time of 12.855 min (Figure 18) with smaller peaks seen at retention times of 14.135 min (Figure 19) and 14.290 min (Figure 20). The mass spectra of all three peaks contained peaks at 207 m/z fragments. Again, no peaks were observed with mass of 423 m/z. No major peaks were observed above 281 m/z.

The extract was then analyzed using an HP-5MS column where several discernible peaks were seen (Figure 21). Molecular ions of 423 m/z were not observed. Major peaks observed at retention times of 11.850 min (Figure 22) and 16.042 min (Figure 23) did not show any fragments greater than 281 m/z. Compounds with retention times of 16.933 min (Figure 24), 17.042 min (Figure 25) and 17.992 min (Figure 26) exhibited a higher abundance of 207 m/z and 281 m/z and yielded library matches to hexatriacontane (NIST17-2, 96%, 507 g/mol, CAS ID 630-06-8), 16-hentriacontanol (NIST17-1, 94%, 452.8 g/mol, 1070-54-8), and campesterol (SWGDRUG, 82%, 400.7 g/mol, CAS ID 474-62-4) respectively. The peak at 17.300 m/z (Figure 27) exhibited significant peaks at 165 m/z and 430 m/z with abundances of 50% and 25% respectively of in addition to 207 m/z and 281 m/z and yielded a library (SWGDRUG)

match of alpha-tocopherol (93%, 430.7 g/mol, CAS ID 1406-18-4). The peak seen at 18.617 min (Figure 28) exhibited major m/z peaks at 207 m/z and 281 m/z as seen with the other peaks of the chromatograms and yielded a library (NIST17) match to gamma-sitosterol (90%, 432.7 g/mol, CAS ID 6131-86-8).

Sitosterol and campesterol are both common sterols found in plants. Additionally, campesterol is a major component in the biosynthesis pathway of brassinosteroids found in Brassica plants such as kale (Srivastava, 2002) (Iva Pavlović, 2018). Therefore, it is plausible that the identity of the target compound is one of these compounds, or a similar compound in the brassinosteroid biosynthesis pathway.

LC-MS/MS

In an attempt to identify if any fragmentation patterns seen in GC-MS could be attributed to the target compound, the kale extract was analyzed using LC-MS/MS. Initially, the same column used for the HPLC analysis was used with the same solvent system for a direct comparison. However, this column and flow rate were not compatible with the instrument setup. Therefore, a different C18 column was used with a gradient mobile phase. This resulted in several overlapping peaks eluting between 2.5 min and 8 min (Figure 29). Mass spectra collected at different retention times (Figure 30, Figure 31, Figure 32) were not consistent with those observed from GC-MS profiles. Furthermore, these spectra were searched in the Mass Bank High Quality Spectral Database (Consortium, 2021) and no matches greater than 43% were found. Therefore, further work is needed to optimize the LC-MS/MS analysis for better peak separation and identification of mass fragments present.

Conclusions

In this study, the identity of the compound causing red autofluorescence in touch samples after handling kale was investigated. It was determined that the compound was intrinsic to the kale itself and not a compound added to the surface of the kale. Through analysis with DART-MS at different voltages, it was evident that the structure of the target compound was resistant to fragmentation or resulted in a very stable fragment at 423.45 m/z. Additionally, when compared to gluconasturtiin and glucoiberin, which both have similar masses to the 423 m/z seen in the DART-MS, it was seen that the structure of the target compound was more resistant to fragmentation. This in combination with the difference in the fluorescence seen between the target compound the gluconasturtiin indicated that the target compound may not be related to glucosinolate compounds. Instead, when a library search was performed on the DART-MS data of the target compound, a library match of 22-desoxycarpesterol was found. Additionally, library matches of gamma-sitosterol and campesterol were found when the kale extract was analyzed using GC-MS. This indicates that the target compound could potentially be a sterol. This is supported by the fact that campesterol is a major component of the brassinosteroid biosynthesis of many *Brassica* plants including kale. To confirm the identity of the target compound further analysis is still needed. Analysis with LC-MS/MS was employed to attempt to match one or more of the fragmentation patterns seen with GC-MS to the target compound, however, matching patterns were not seen. Additionally, library matches were not found for the fragmentation patterns seen with LC-MS/MS. Therefore, further optimization is needed to isolate the target compound and determine its fragmentation pattern. This could ideally allow the identification of the compound, though further characterization may be required.

Figures

Figure 1

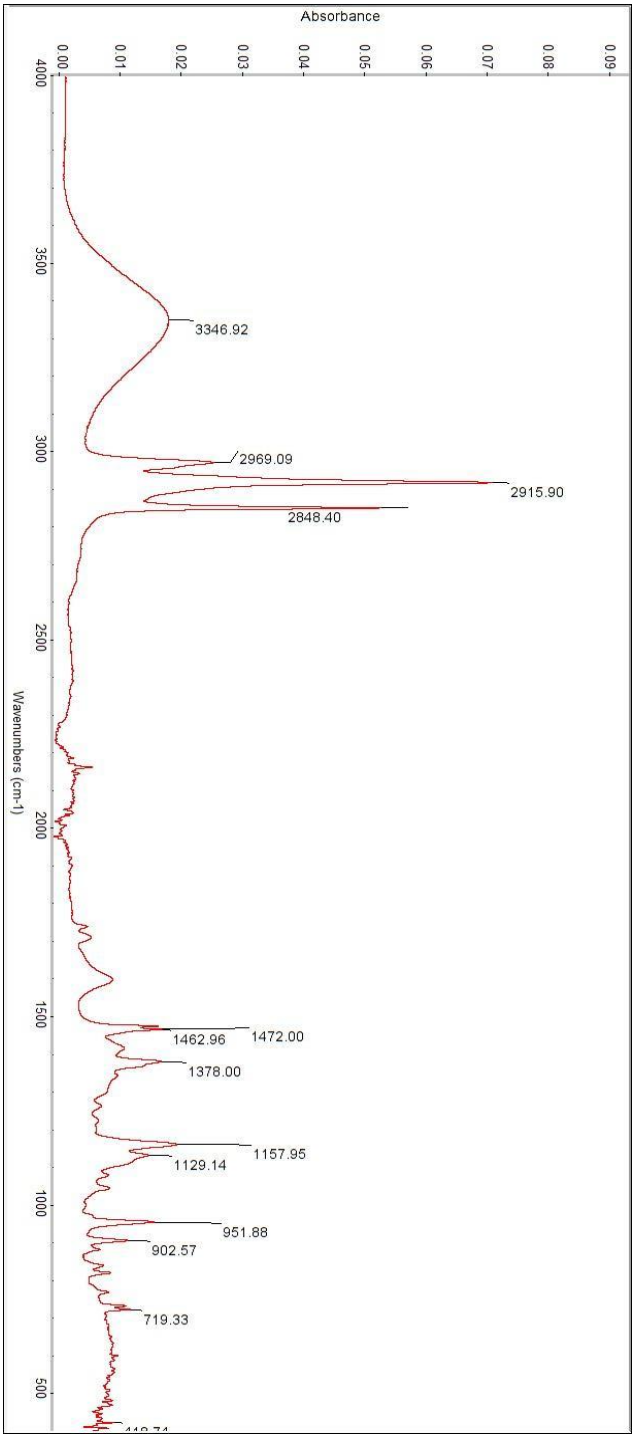

Figure 1. FTIR spectrum of kale extract.

Figure 2

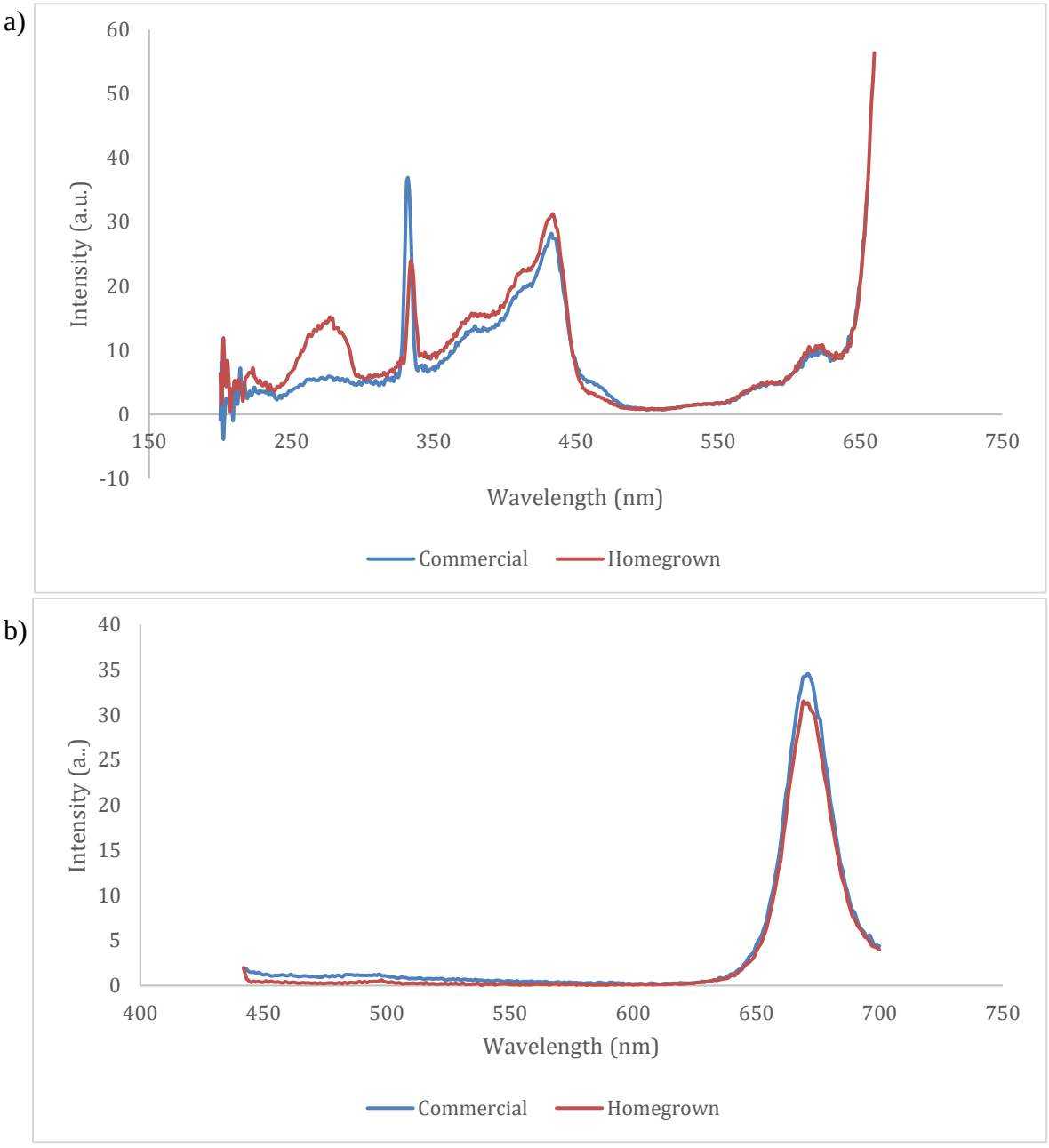

Figure 2. a) Excitation scan of kale extracts of both homegrown kale and commercial kale at emission wavelengths of 670 nm and 665 nm respectively. b) Emission scan of kale extracts of both homegrown and store-bought kale at excitation wavelengths of 434 nm and 432 nm respectively.

Figure 3

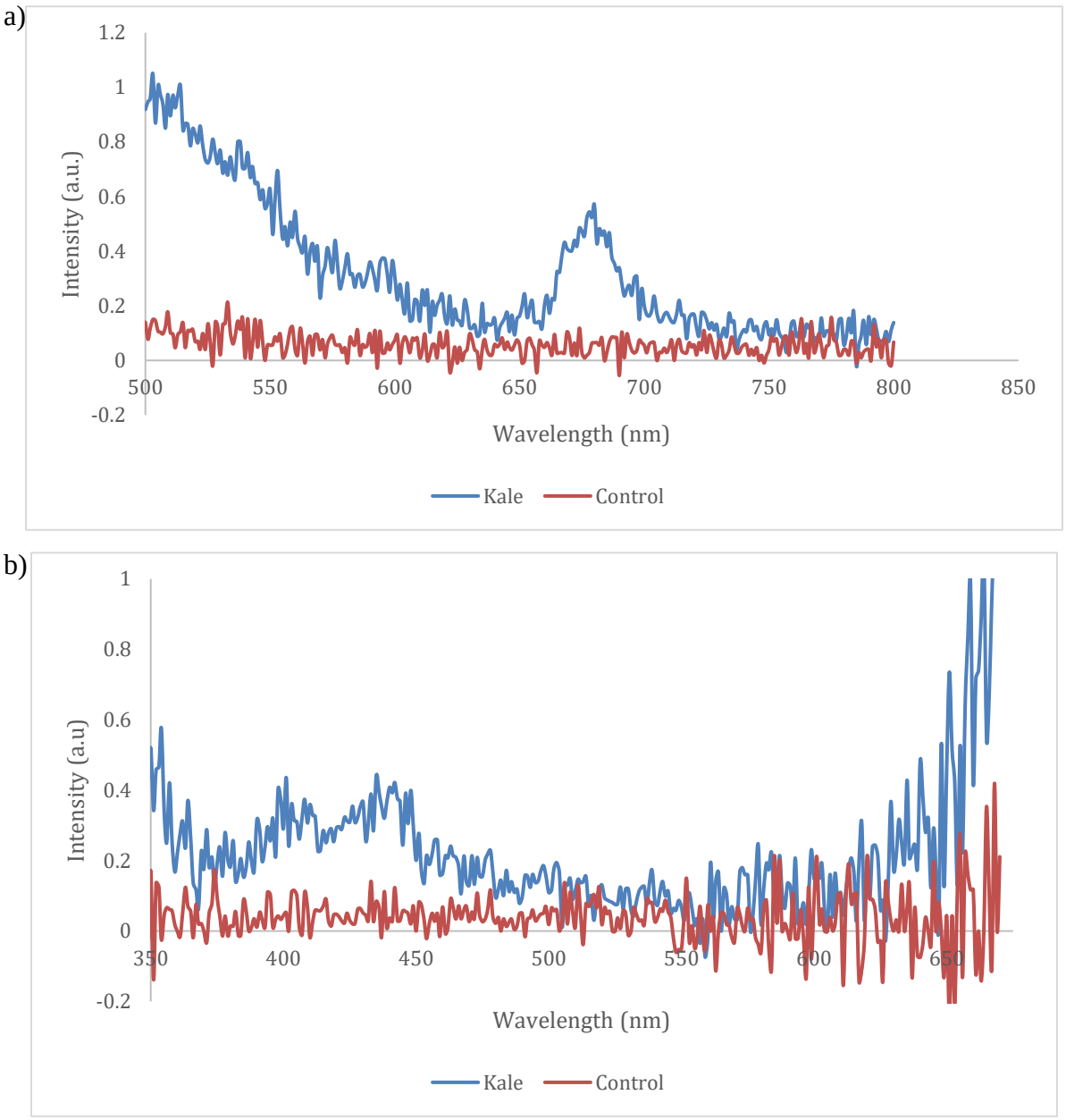

Figure 3. a) Emission scan of touch samples after handling kale and control touch samples with an excitation wavelength of 435 nm. b) Excitation scan of touch samples after handling kale and control touch samples with an emission wavelength of 680 nm.

Figure 4

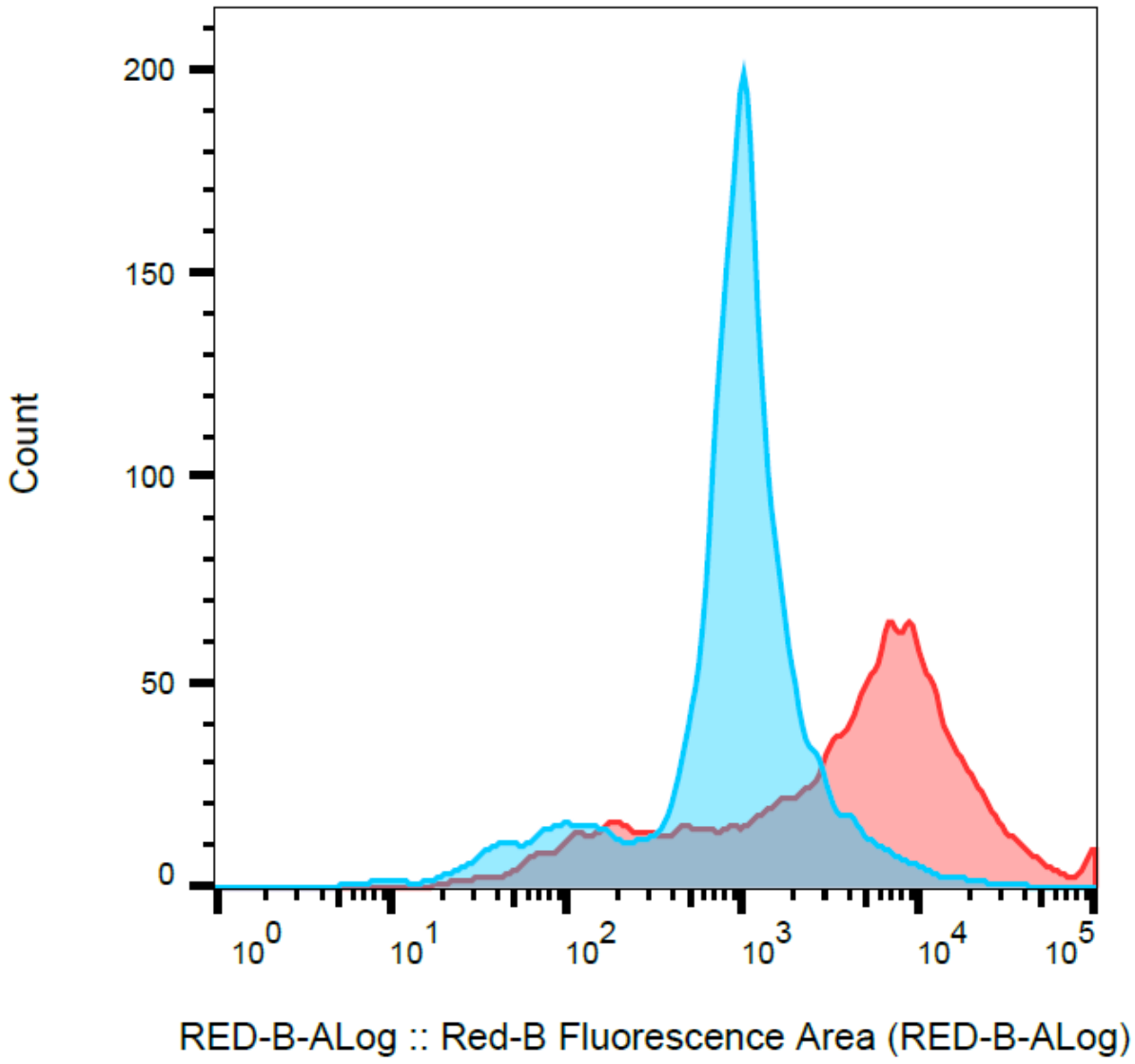

	Sample Name	Subset Name	Count
	009-edw-200923_control.fcs	large cells	5469
	009-edw-200923_kale.fcs	large cells	4052

Figure 4. Histograms of the fluorescence in the red channel of both control touch samples and touch samples after handling kale after analysis with flow cytometry.

Figure 5

a)

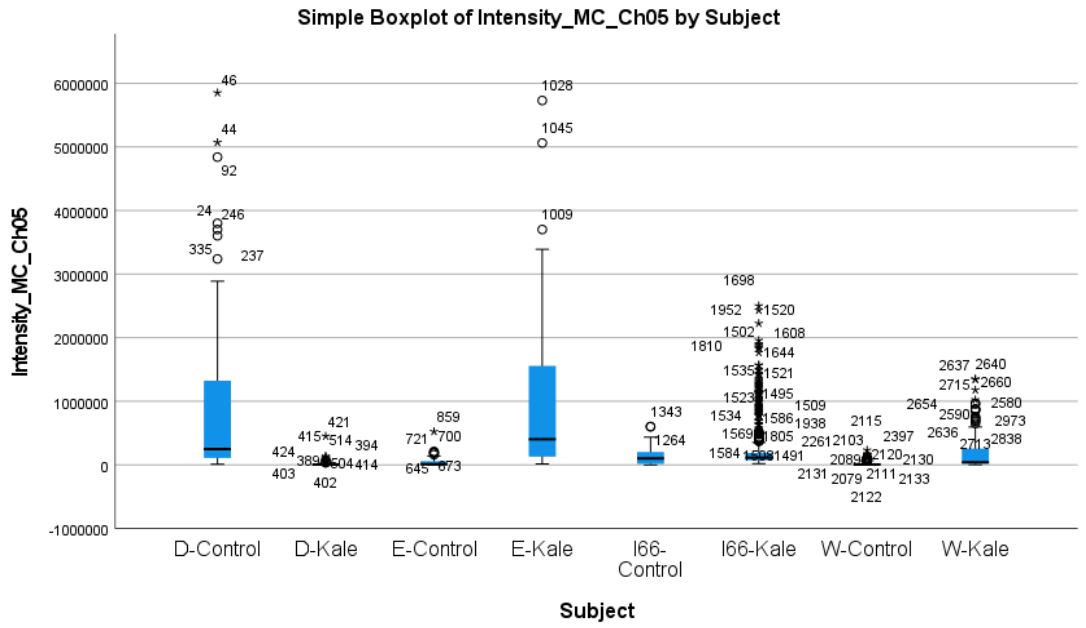

b)

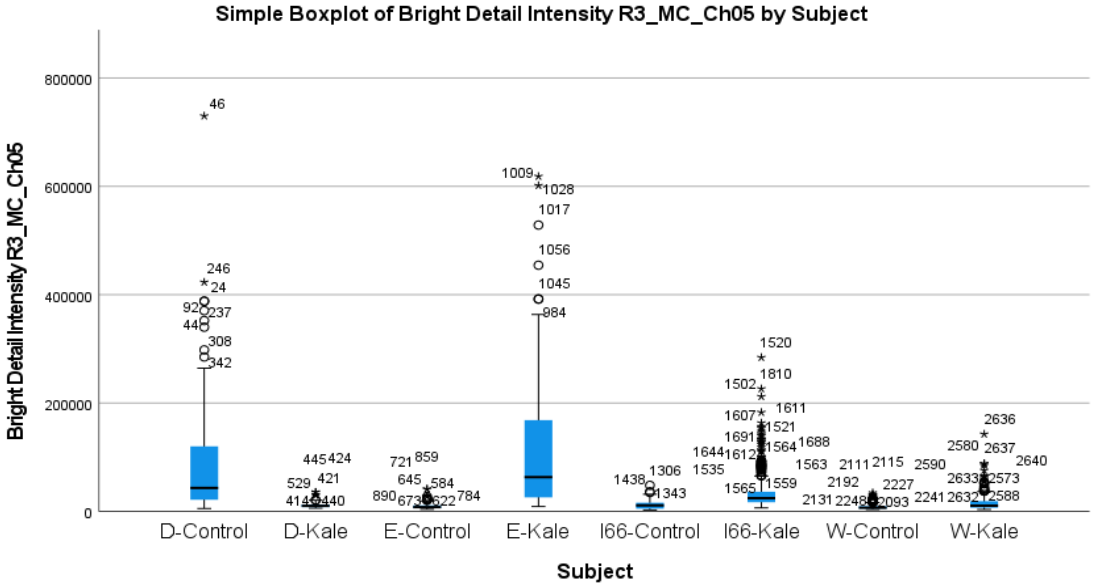

Figure 5. a) Box plot comparing the intensity of the fluorescence seen in the red channel with imaging flow cytometry of control touch samples and touch samples after handling kale. Box plot comparing the intensity of the bright detail seen in the red channel with imaging flow cytometry of control touch samples and touch samples after handling kale.

Figure 6

a)

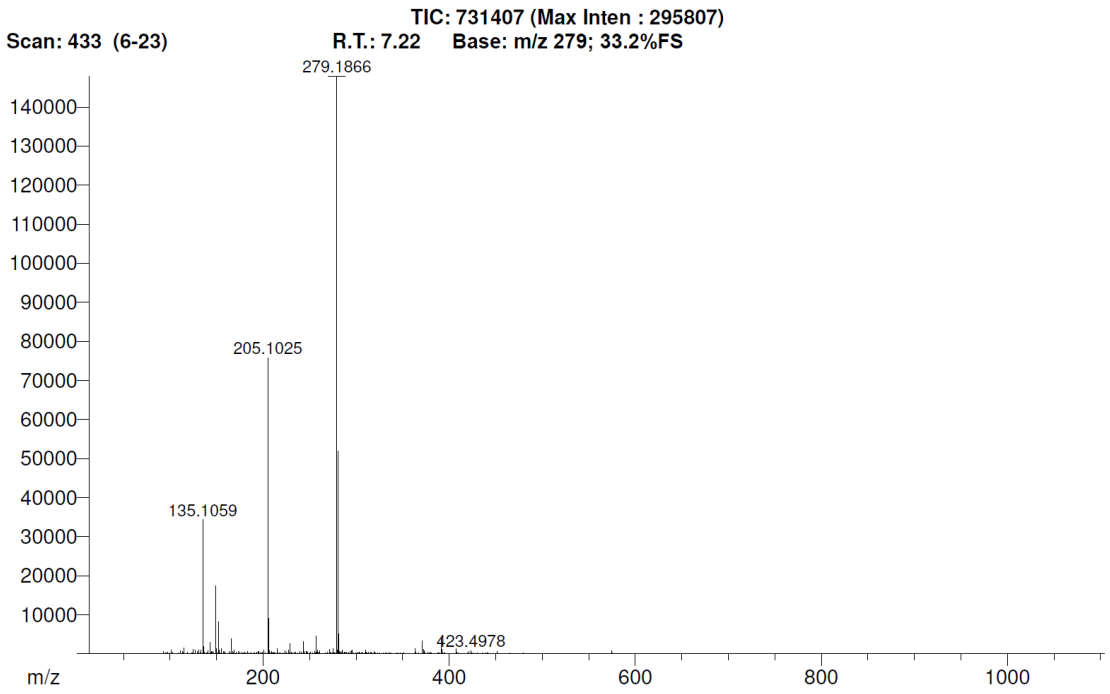
TIC: 731407 (Max Inten : 295807)
Scan: 433 (6-23)
R.T.: 7.22
Base: m/z 279; 33.2%FS
279.1866
205.1025
135.1059
423.4978
m/z

b)

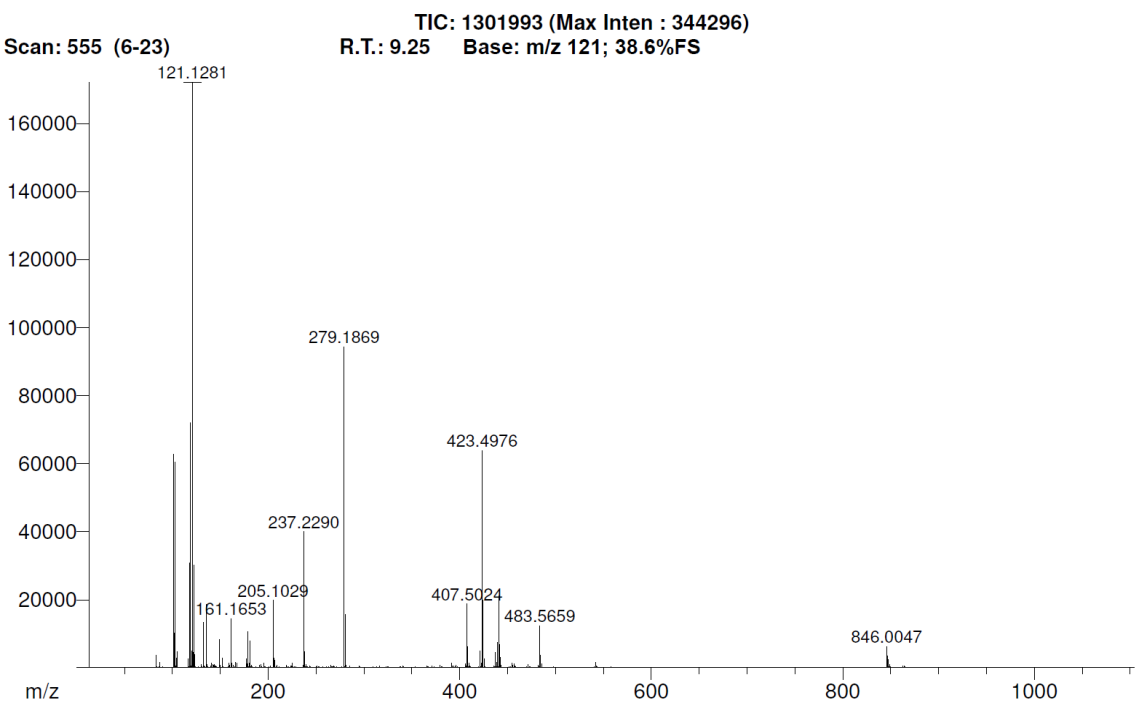
TIC: 1301993 (Max Inten : 344296)
Scan: 555 (6-23)
R.T.: 9.25
Base: m/z 121; 38.6%FS
121.1281
279.1869
423.4976
237.2290
205.1029
161.1653
407.5024
483.5659
846.0047
m/z

c)

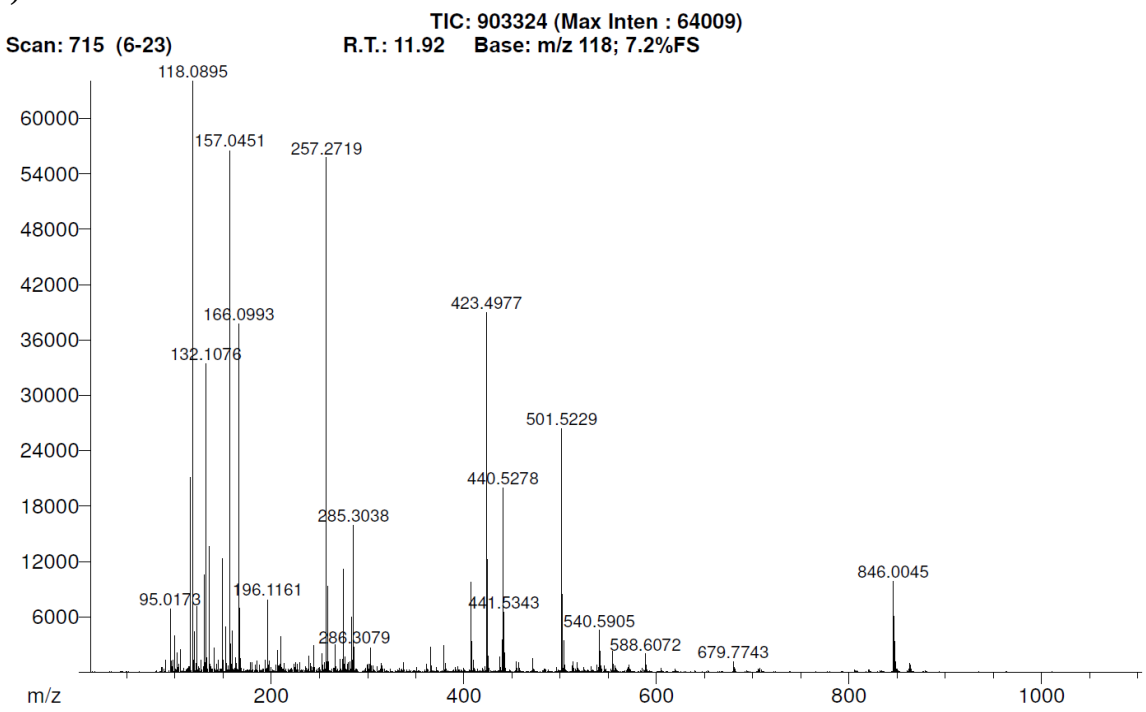

Figure 6. DART-MS mass spectrum of a) touch samples after handling kale, b) kale extract, and c) the kale leaf at 20V in positive mode.

Figure 7

a)

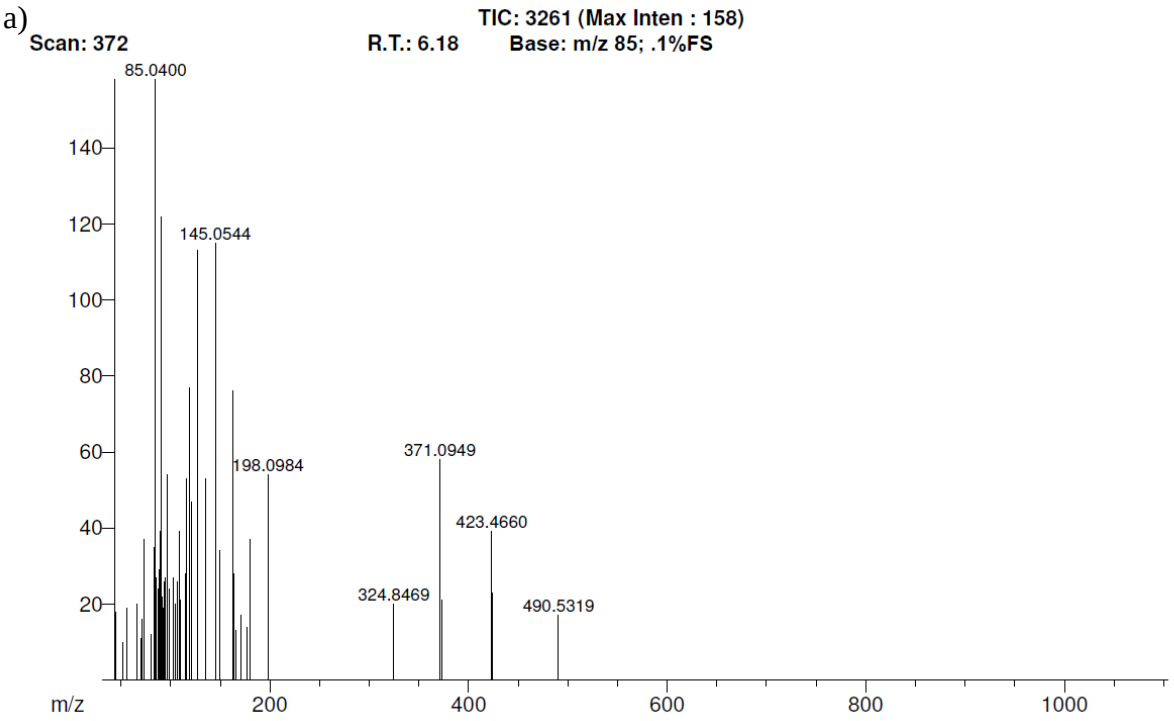
TIC: 3261 (Max Inten : 158)
Scan: 372
R.T.: 6.18
Base: m/z 85; .1%FS
85.0400
145.0544
198.0984
371.0949
423.4660
324.8469
490.5319
m/z

b)

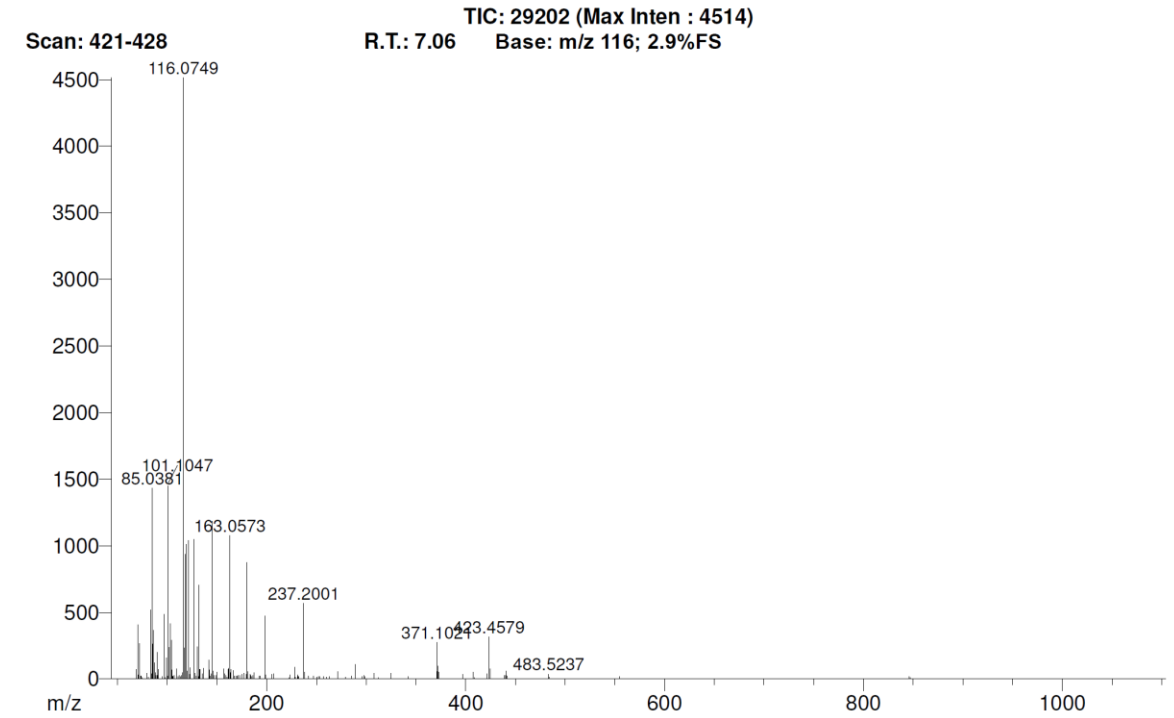
TIC: 29202 (Max Inten : 4514)
Scan: 421-428
R.T.: 7.06
Base: m/z 116; 2.9%FS
116.0749
101.1047
85.0381
163.0573
237.2001
371.1021
423.4579
483.5237
m/z

c)

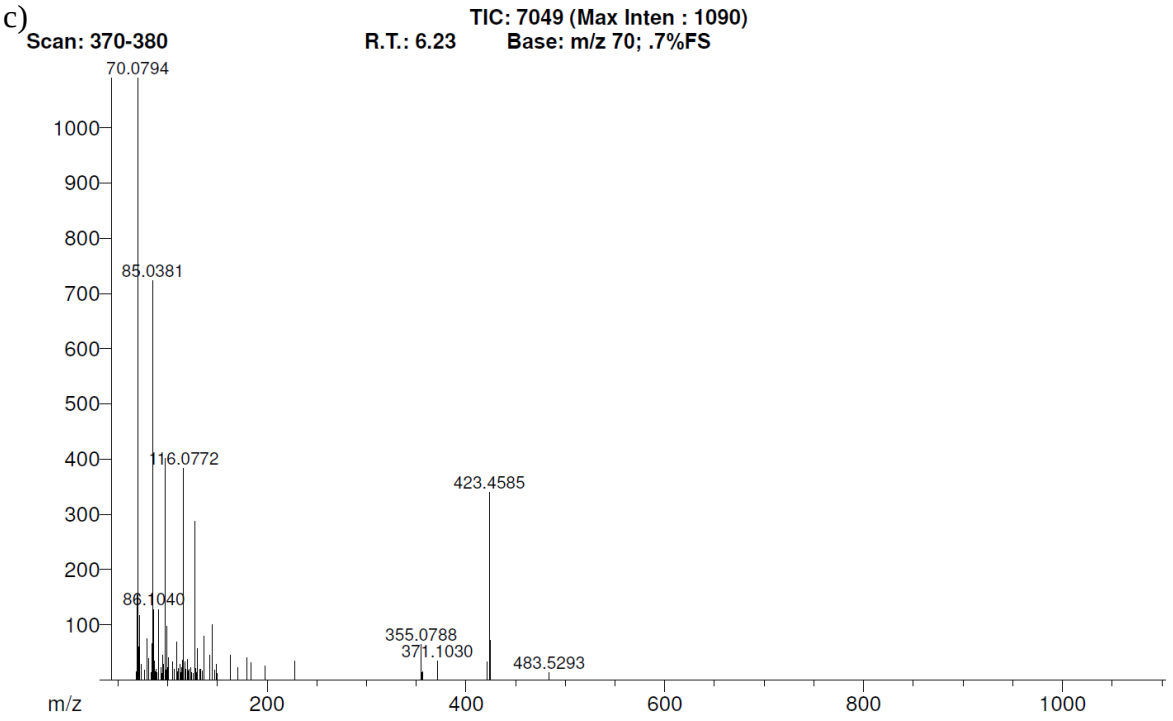
TIC: 7049 (Max Inten : 1090)
Scan: 370-380
R.T.: 6.23
Base: m/z 70; .7%FS
70.0794
85.0381
116.0772
423.4585
86.1040
355.0788
371.1030
483.5293
m/z
200
400
600
800
1000

d)

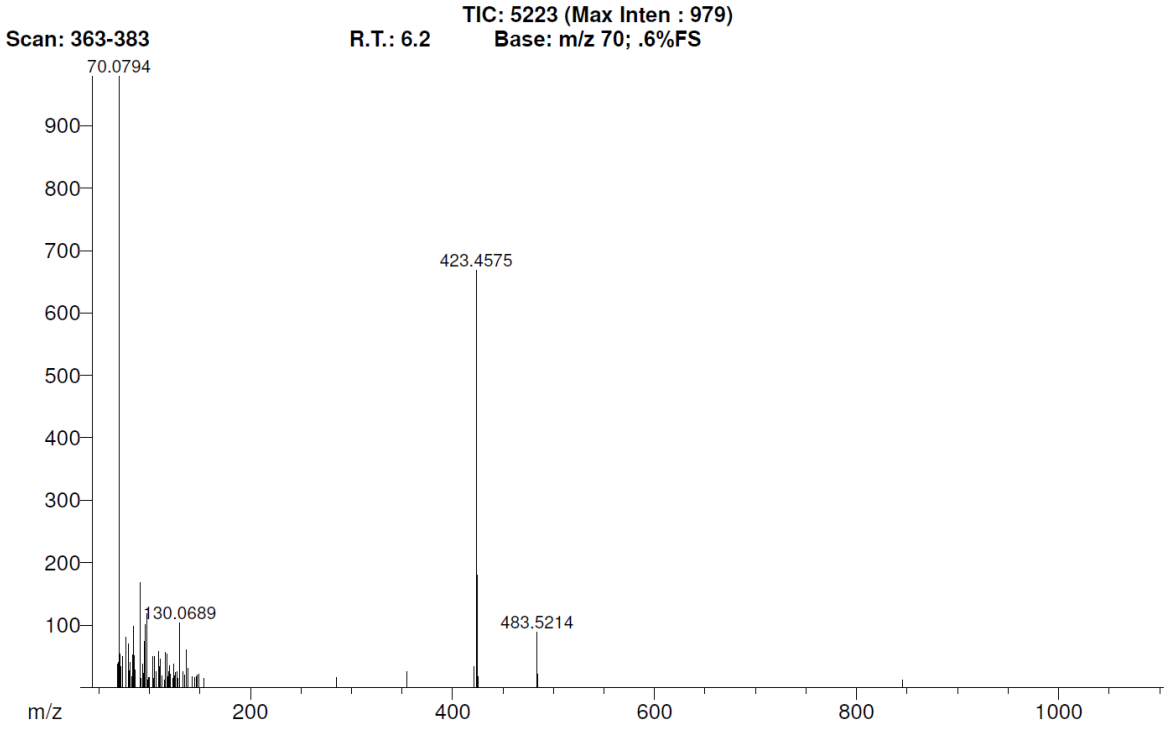
TIC: 5223 (Max Inten : 979)
Scan: 363-383
R.T.: 6.2
Base: m/z 70; .6%FS
70.0794
423.4575
130.0689
483.5214
m/z
200
400
600
800
1000

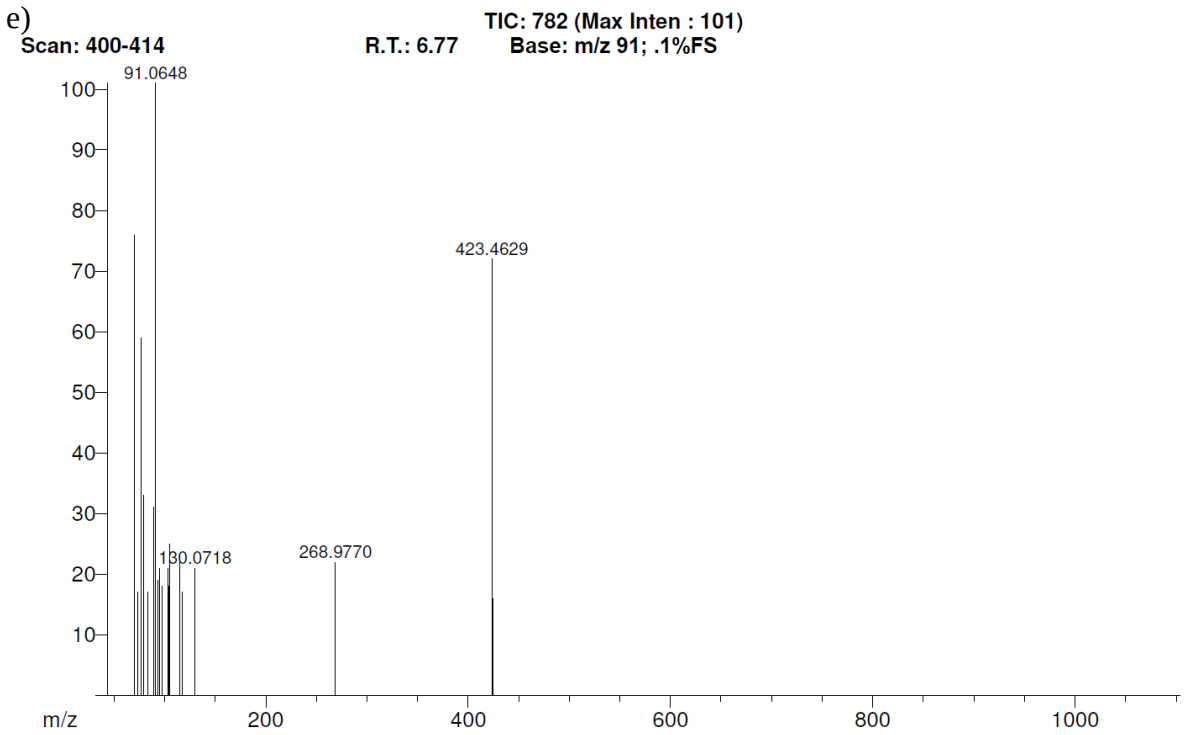

Figure 7. DART-MS mass spectrum of the kale extract in isopropanol in positive mode at a) 20V, b) 30V, c) 60V, d) 90V, and e) 120V.

Figure 8

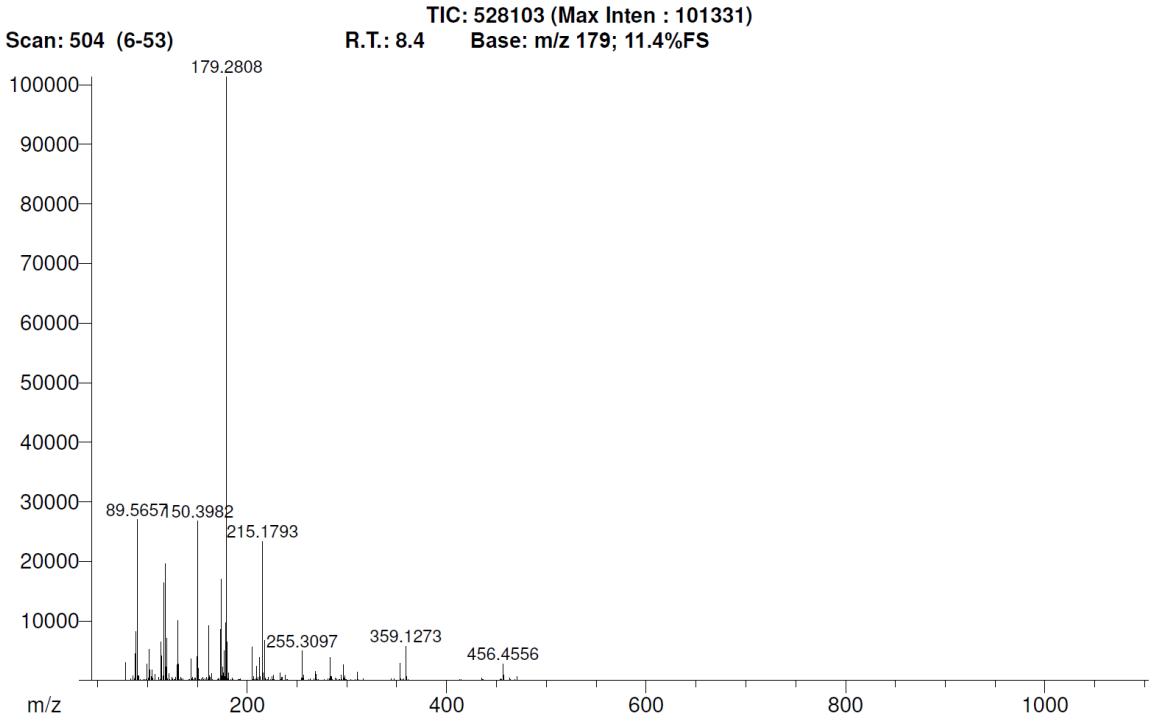

Figure 8. DART-MS mass spectrum of the kale extract in isopropanol at 20V in negative mode.

Figure 9

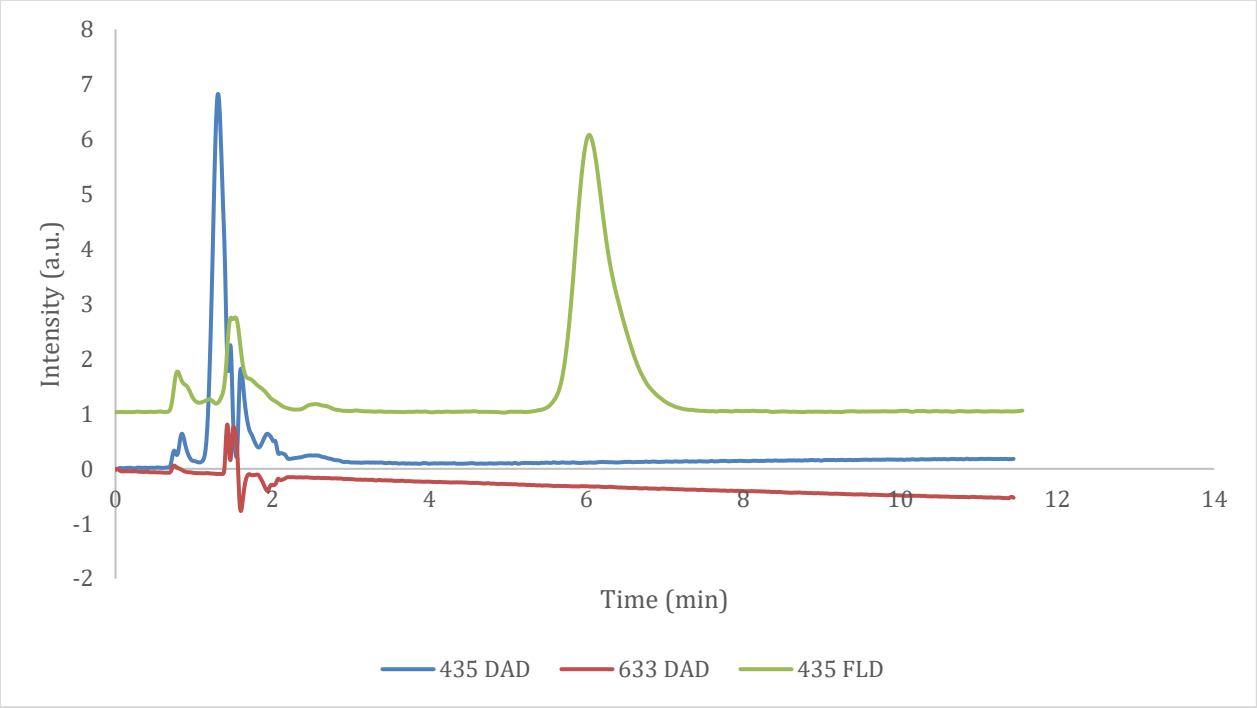

Figure 9. HPLC chromatograph of kale extract with a diode array detector at 435 nm and 633 nm as well as a fluorescence detector at 435 nm.

Figure 10

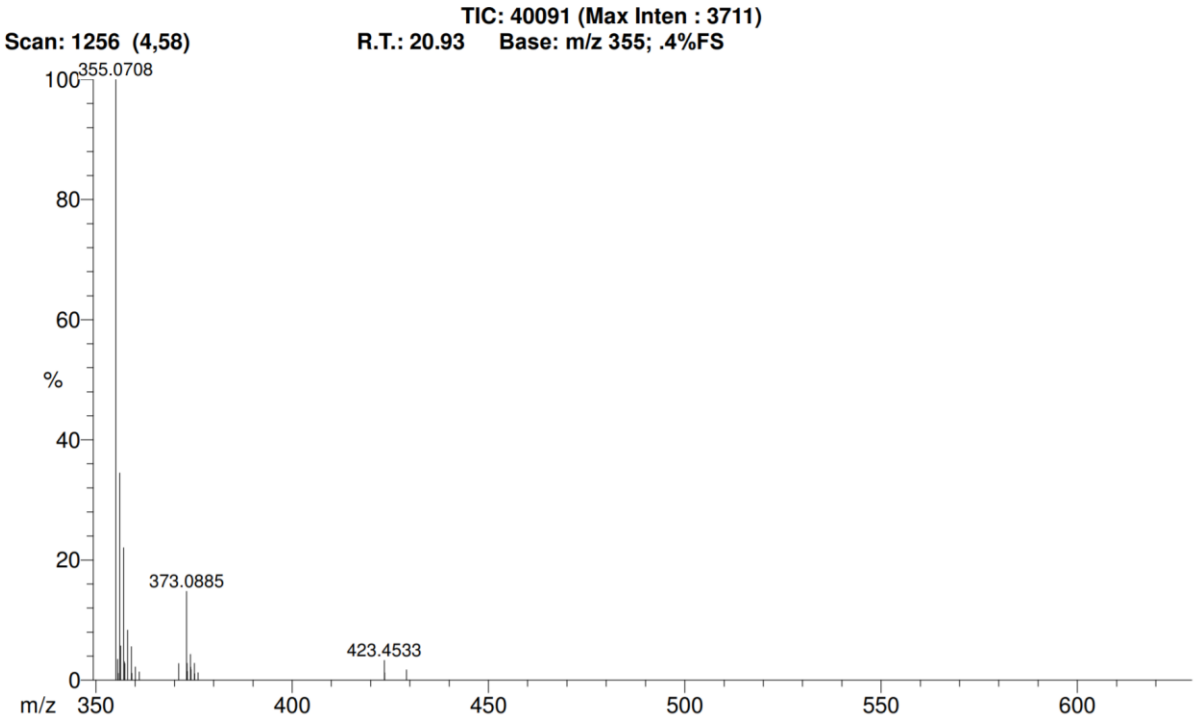

Figure 10. DART-MS mass spectrum of fraction collected from HPLC separation of the collared green extract.

Figure 11

a)

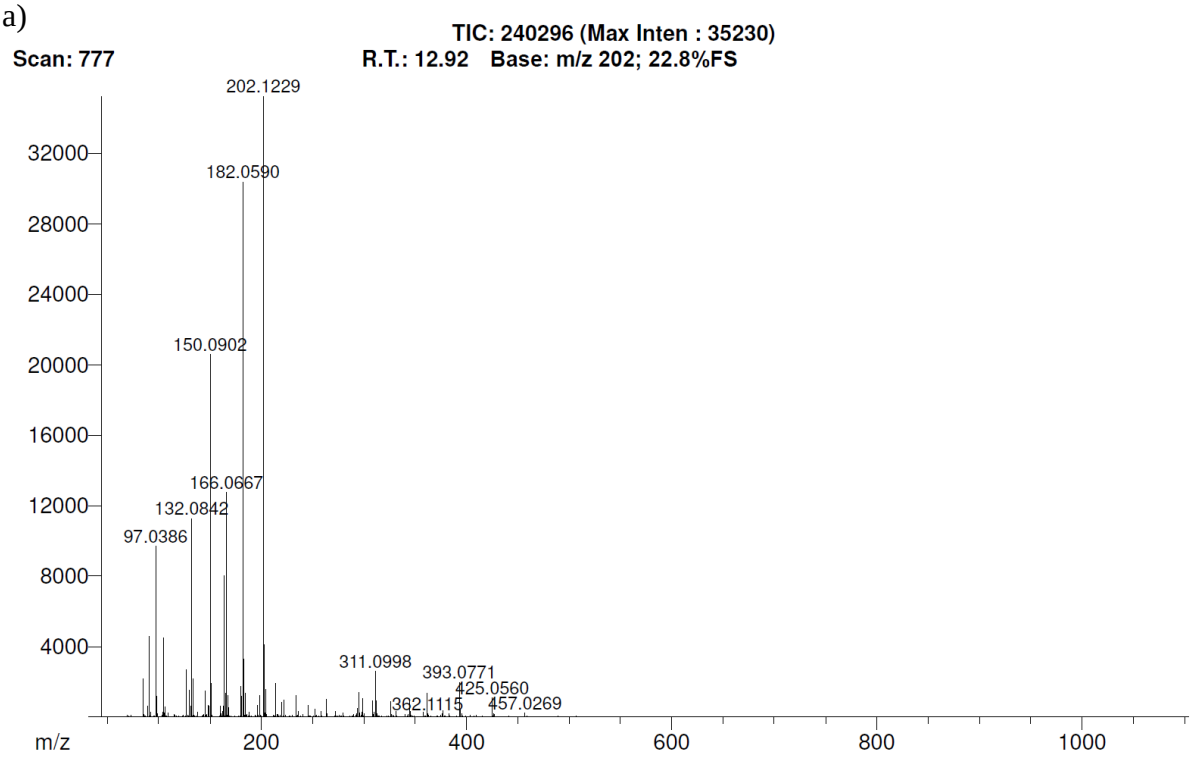
TIC: 240296 (Max Inten : 35230)
Scan: 777
R.T.: 12.92 Base: m/z 202; 22.8%FS
202.1229
182.0590
150.0902
166.0667
132.0842
97.0386
311.0998
393.0771
425.0560
362.1115
457.0269
32000
28000
24000
20000
16000
12000
8000
4000
m/z
200
400
600
800
1000

b)

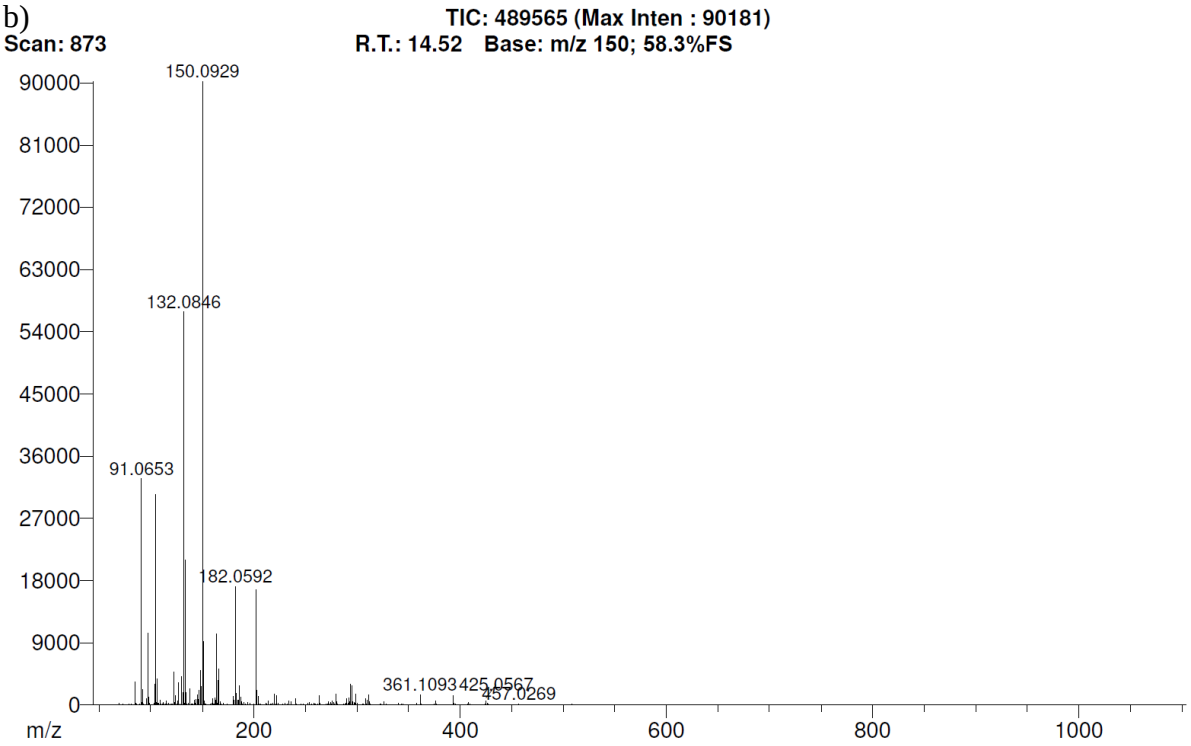
TIC: 489565 (Max Inten : 90181)
Scan: 873
R.T.: 14.52 Base: m/z 150; 58.3%FS
150.0929
132.0846
91.0653
182.0592
361.1093
425.0567
457.0269
90000
81000
72000
63000
54000
45000
36000
27000
18000
9000
0
m/z
200
400
600
800
1000

c)

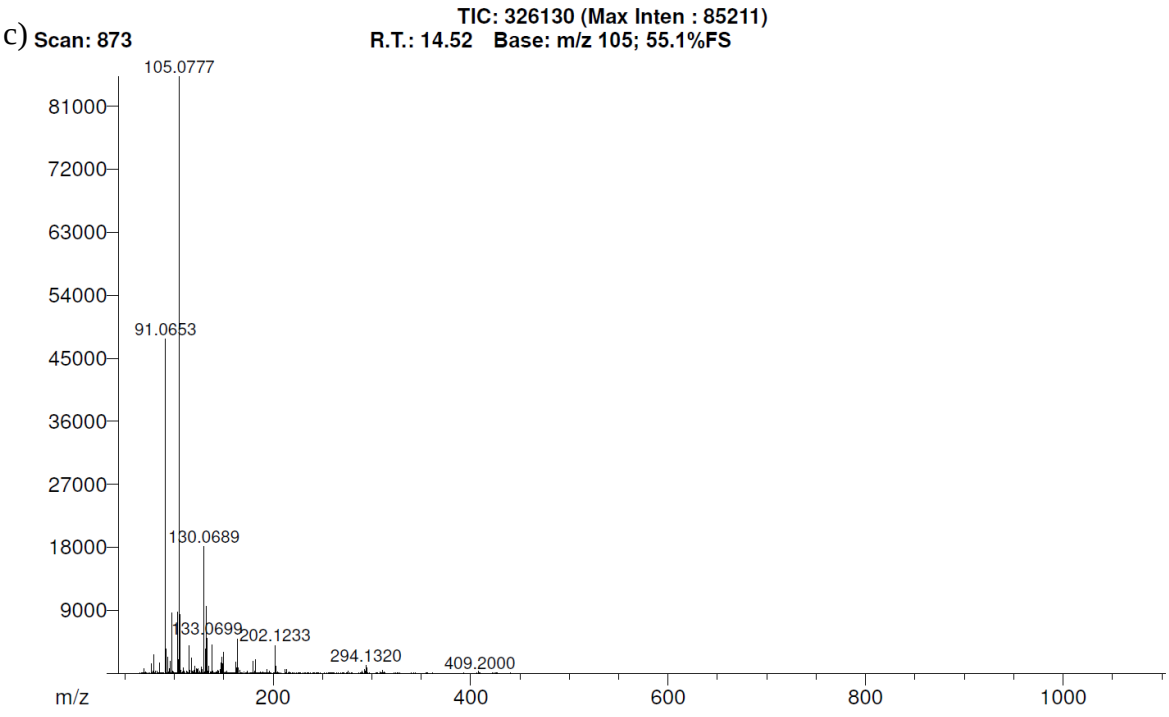
TIC: 326130 (Max Inten : 85211)
Scan: 873
R.T.: 14.52 Base: m/z 105; 55.1%FS
105.0777
91.0653
130.0689
133.0699
202.1233
294.1320
409.2000
81000
72000
63000
54000
45000
36000
27000
18000
9000
m/z
200
400
600
800
1000

d)

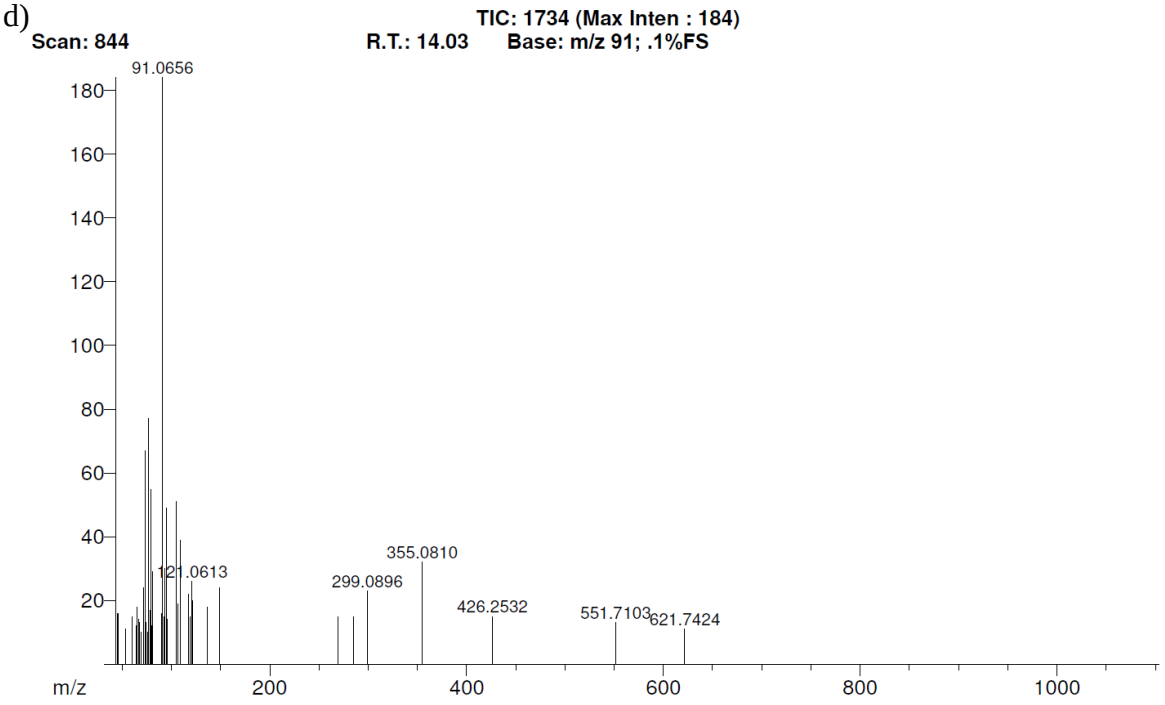
TIC: 1734 (Max Inten : 184)
Scan: 844
R.T.: 14.03 Base: m/z 91; .1%FS
91.0656
121.0613
299.0896
355.0810
426.2532
551.7103
621.7424
180
160
140
120
100
80
60
40
20
m/z
200
400
600
800
1000

e)

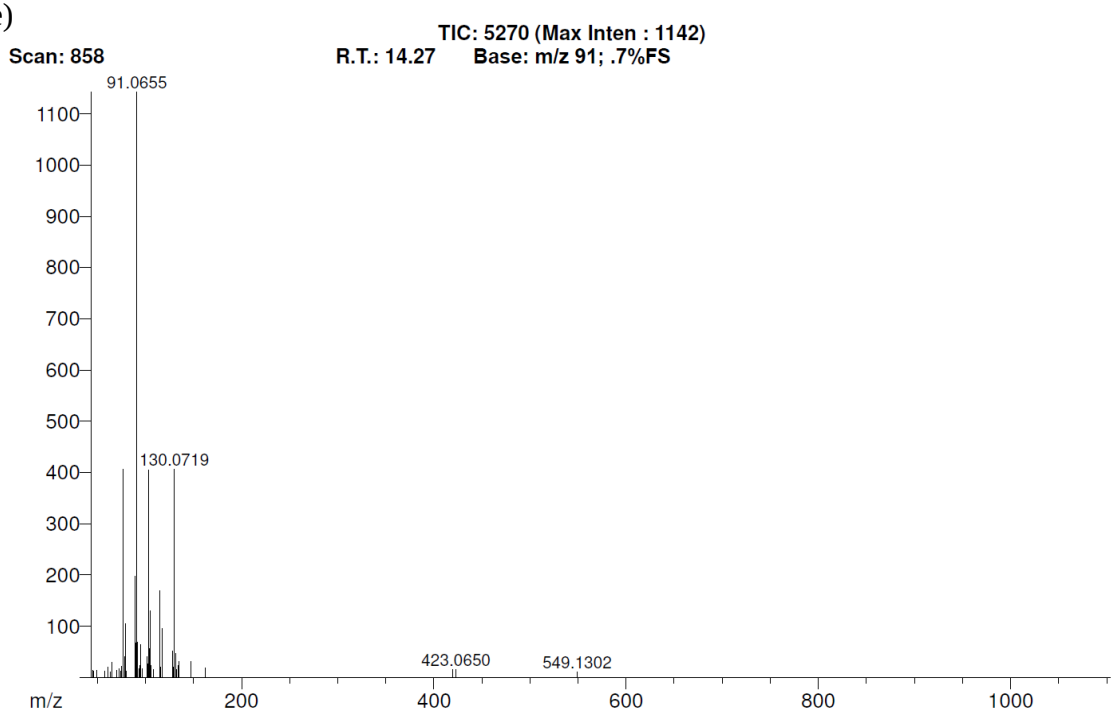

Figure 11. DART-MS mass spectrum of gluconasturtiin at a) 20V, b) 30V, c) 60V, d) 90V, and e) 120V in positive mode.

Figure 12

a)

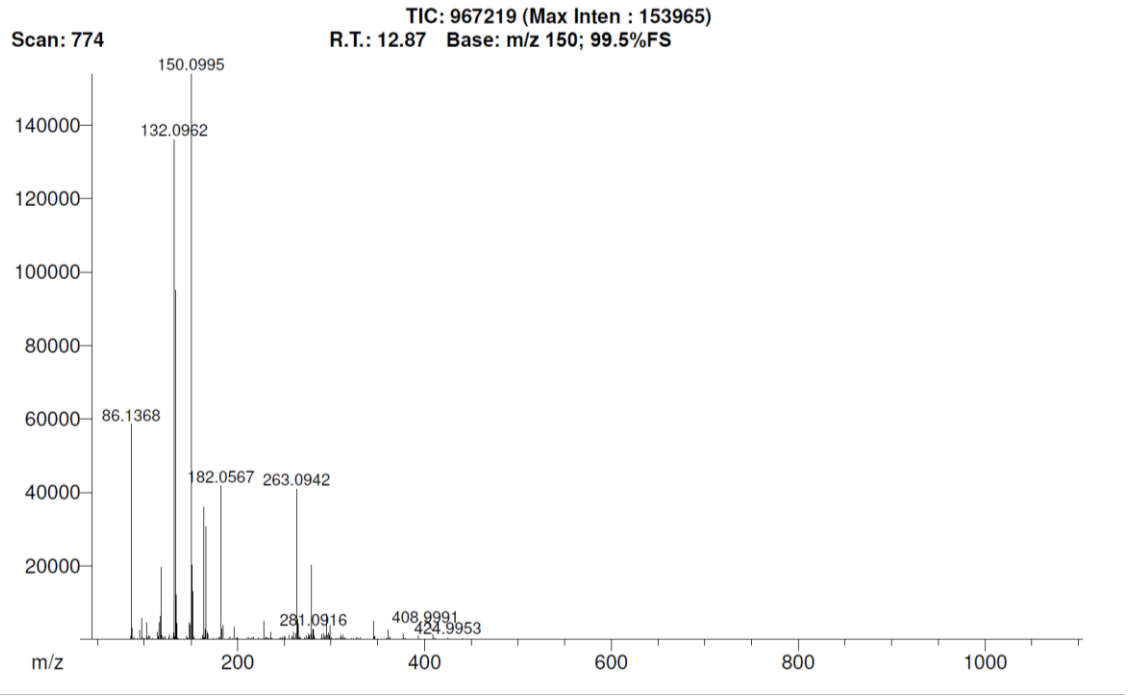
TIC: 967219 (Max Inten : 153965)
Scan: 774
R.T.: 12.87 Base: m/z 150; 99.5%FS
150.0995
132.0962
86.1368
182.0567
263.0942
281.0916
408.9991
424.9953
140000
120000
100000
80000
60000
40000
20000
m/z
200
400
600
800
1000

b)

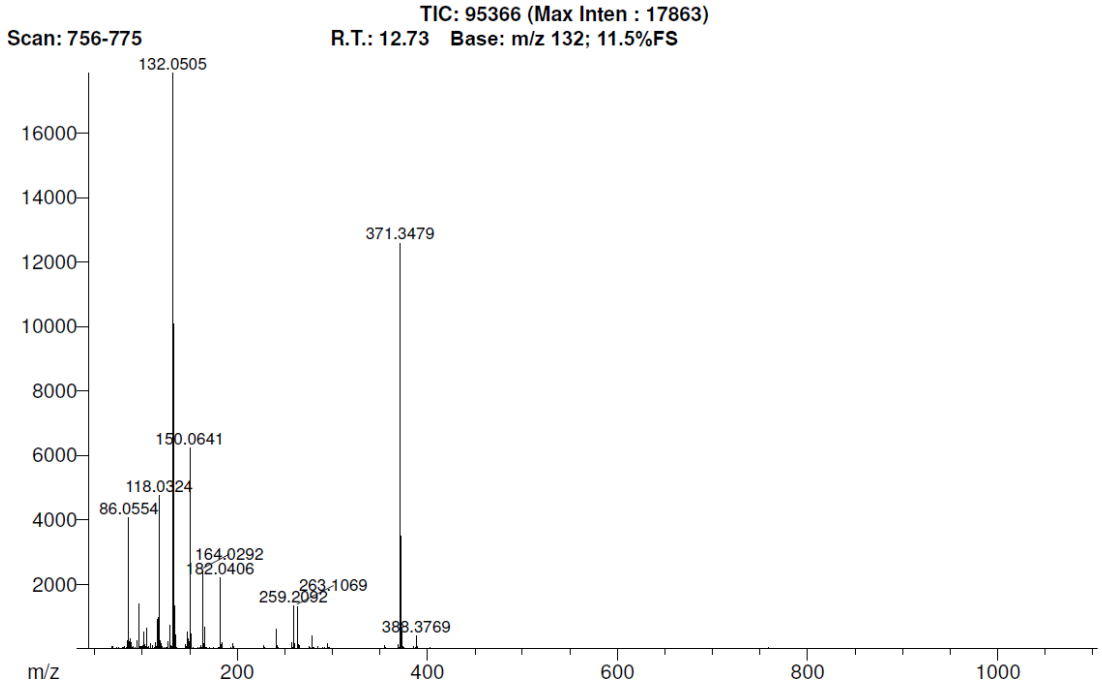
TIC: 95366 (Max Inten : 17863)
Scan: 756-775
R.T.: 12.73 Base: m/z 132; 11.5%FS
132.0505
371.3479
150.0641
118.0324
86.0554
164.0292
182.0406
263.1069
259.2092
383.3769
16000
14000
12000
10000
8000
6000
4000
2000
m/z
200
400
600
800
1000

c)

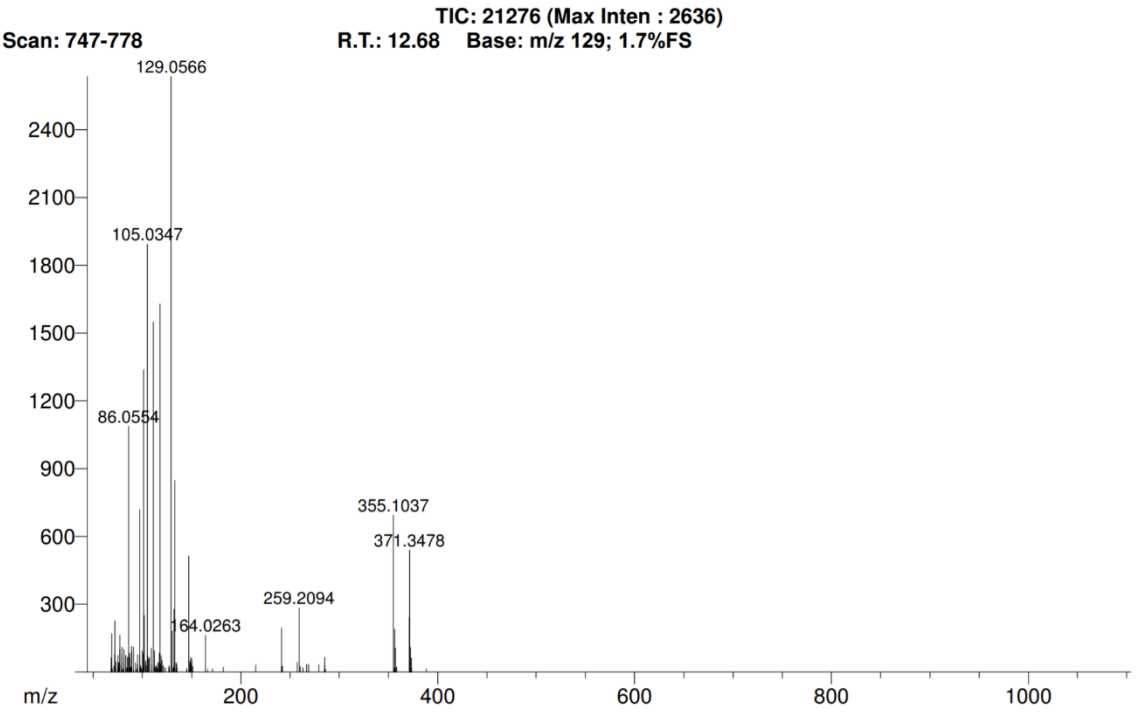
TIC: 21276 (Max Inten : 2636)
Scan: 747-778
R.T.: 12.68
Base: m/z 129; 1.7%FS
129.0566
105.0347
86.0554
355.1037
371.3478
259.2094
164.0263
2400
2100
1800
1500
1200
900
600
300
m/z
200
400
600
800
1000

d)

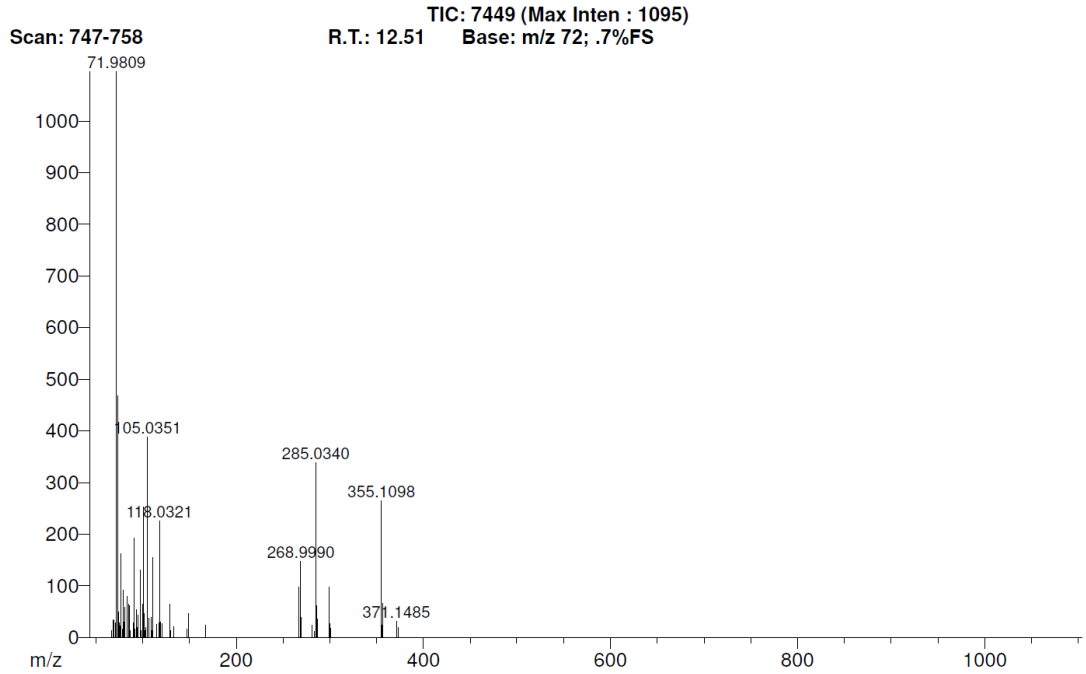
TIC: 7449 (Max Inten : 1095)
Scan: 747-758
R.T.: 12.51
Base: m/z 72; .7%FS
71.9809
105.0351
285.0340
355.1098
118.0321
268.9990
371.1485
1000
900
800
700
600
500
400
300
200
100
0
m/z
200
400
600
800
1000

e)

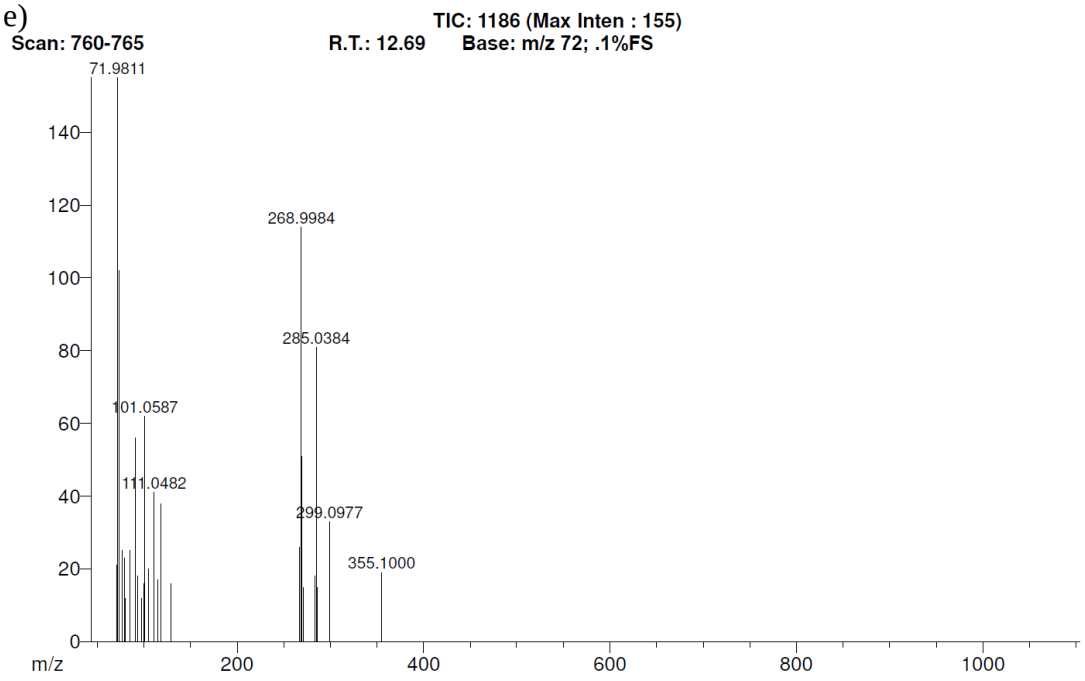

Figure 12. DART-MS mass spectrum of glucoiberin at a) 20V, b) 30V, c) 60V, d) 90V, and e) 120V in positive mode.

Figure 13

a)

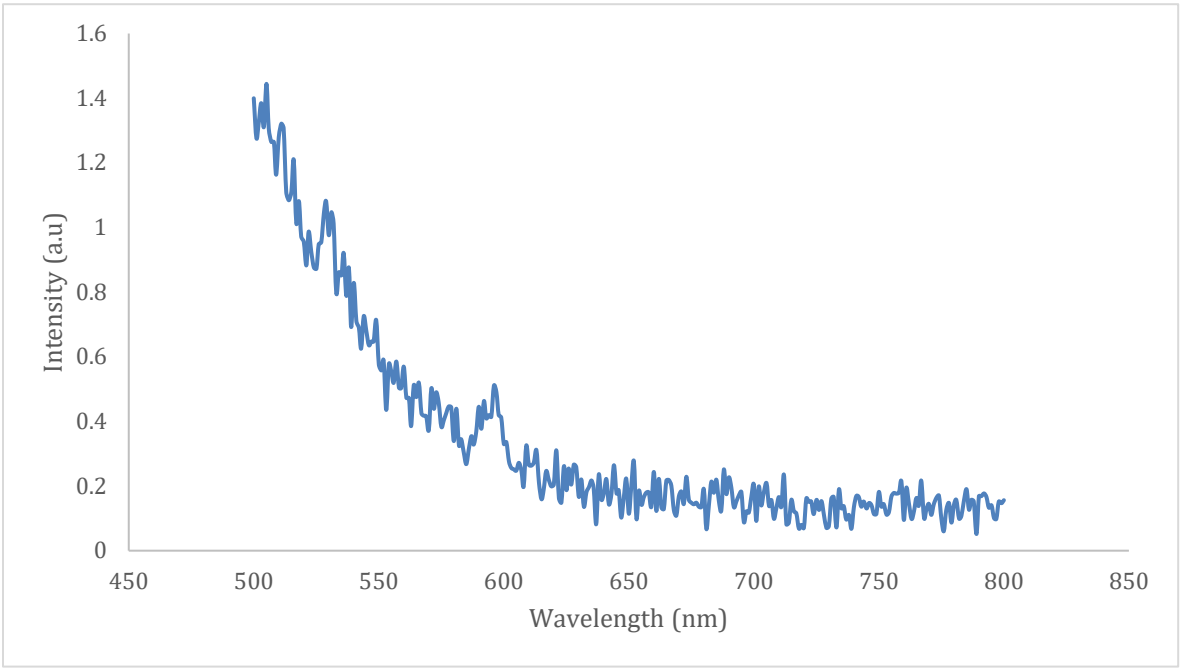

b)

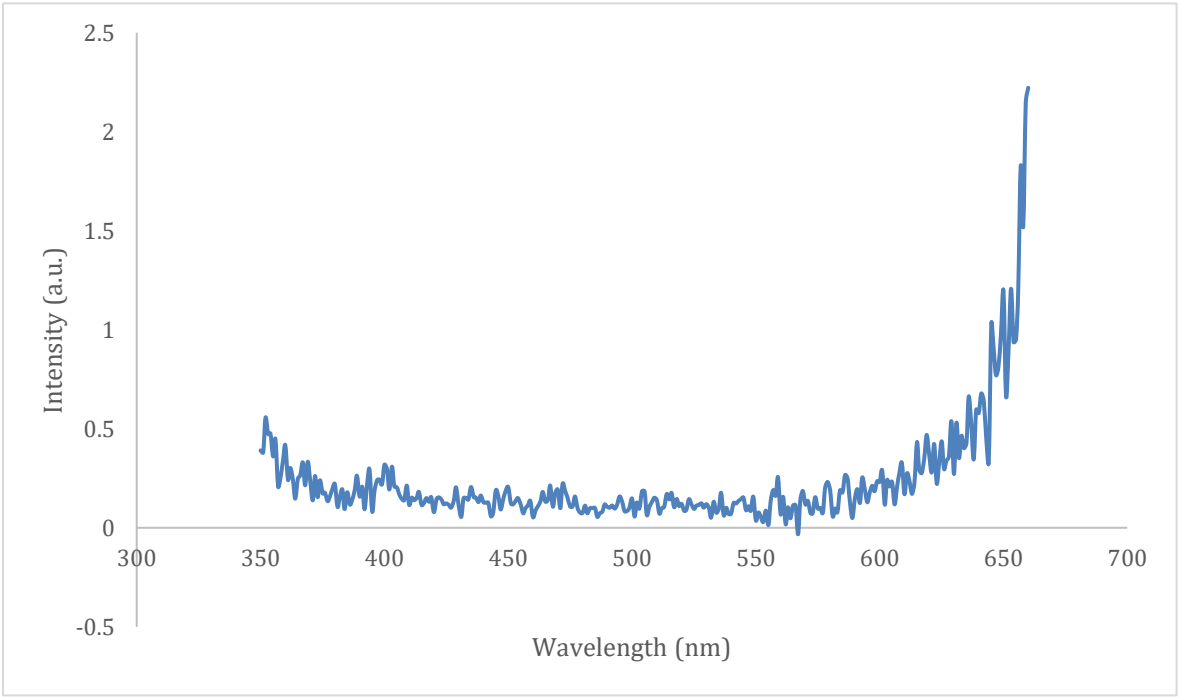

Figure 13. a) Emission scan of gluconasturtiin at an excitation wavelength of 435 nm. b) Excitation scan of gluconasturtiin at an emission wavelength of 670 nm.

Figure 14

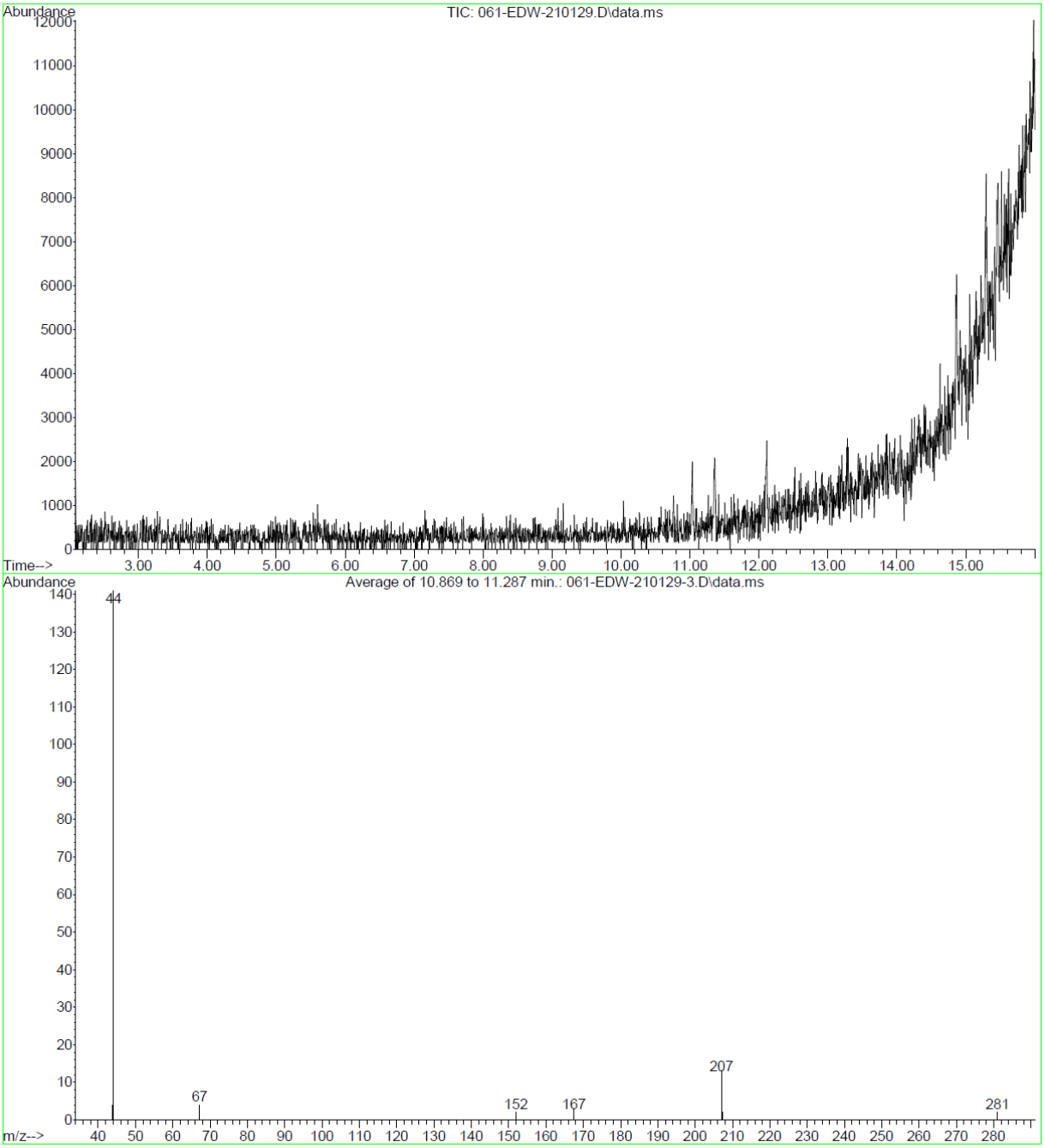

Figure 14. GC-MS chromatogram and mass spectrum performed on an Agilent GC-FID-MS with a DB-1ms column with a 20:1 split.

Figure 15

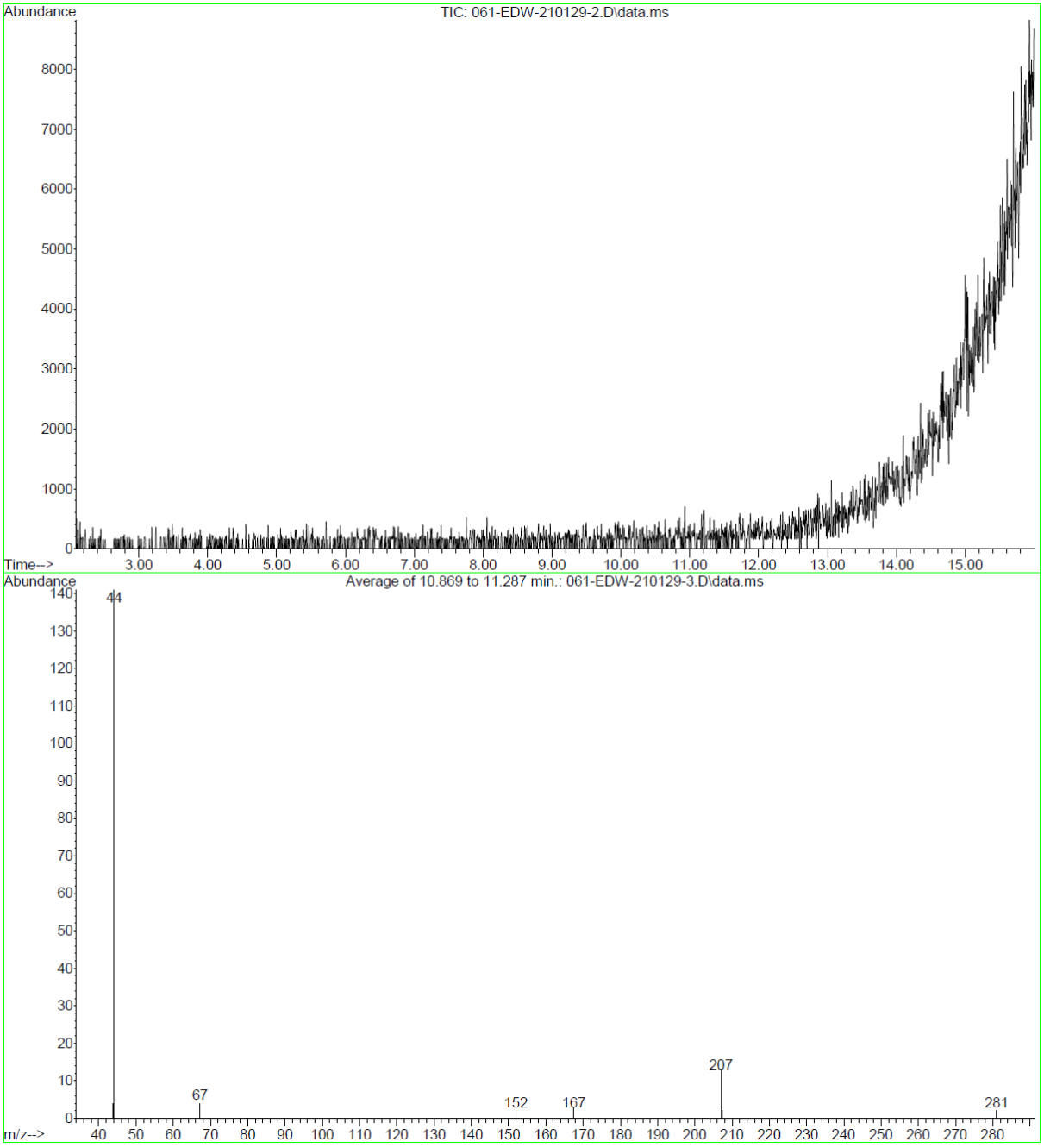

Figure 15. GC-MS chromatogram and mass spectrum performed on an Agilent GC-FID-MS with a DB-1ms column with no split.

Figure 16

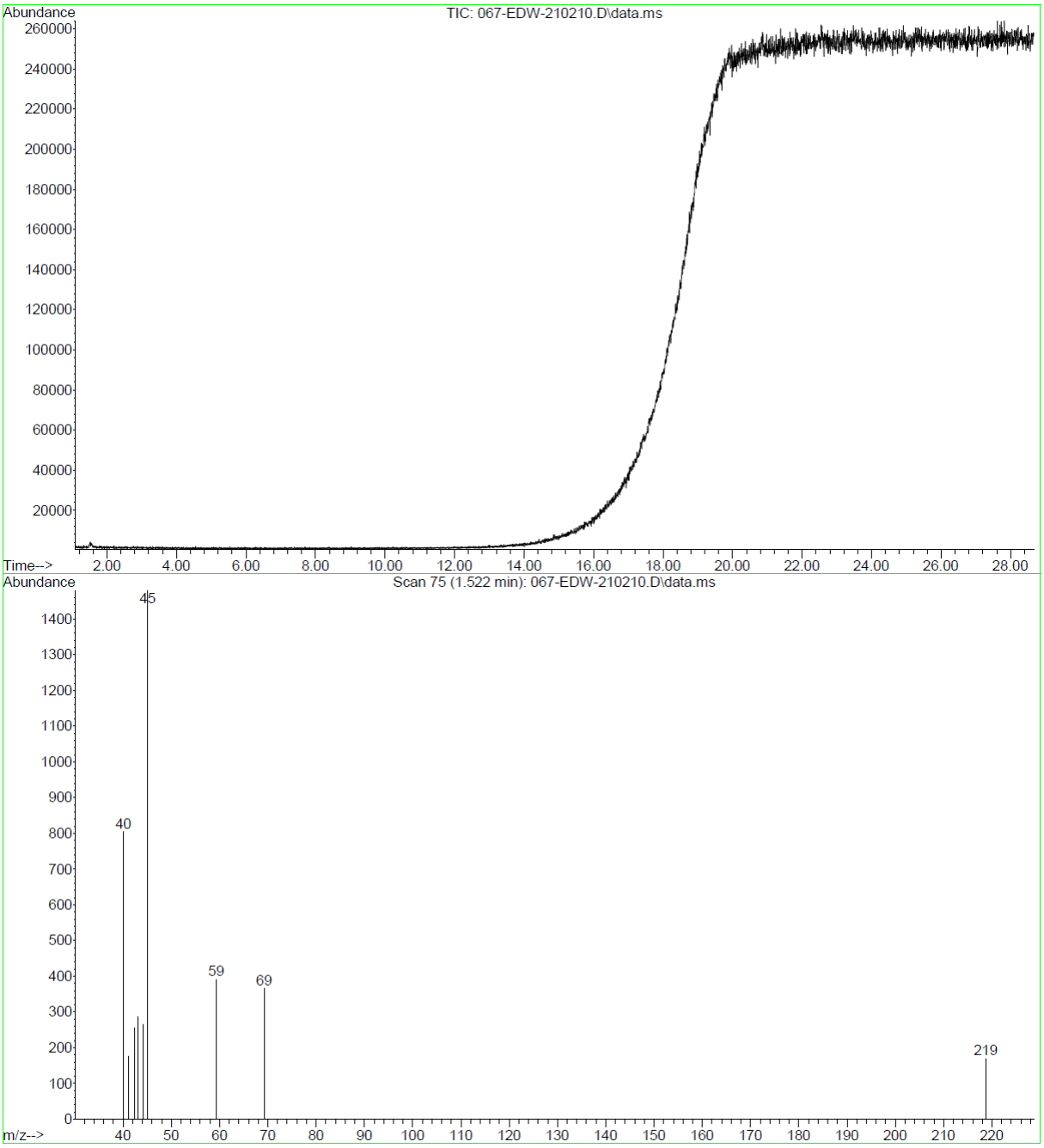

Figure 16. GC-MS chromatogram and mass spectrum performed on an Agilent GC-FID-MS with a DB-1ms column with a ramp rate of 15°C/min and a final oven temperature of 300°C.

Figure 17

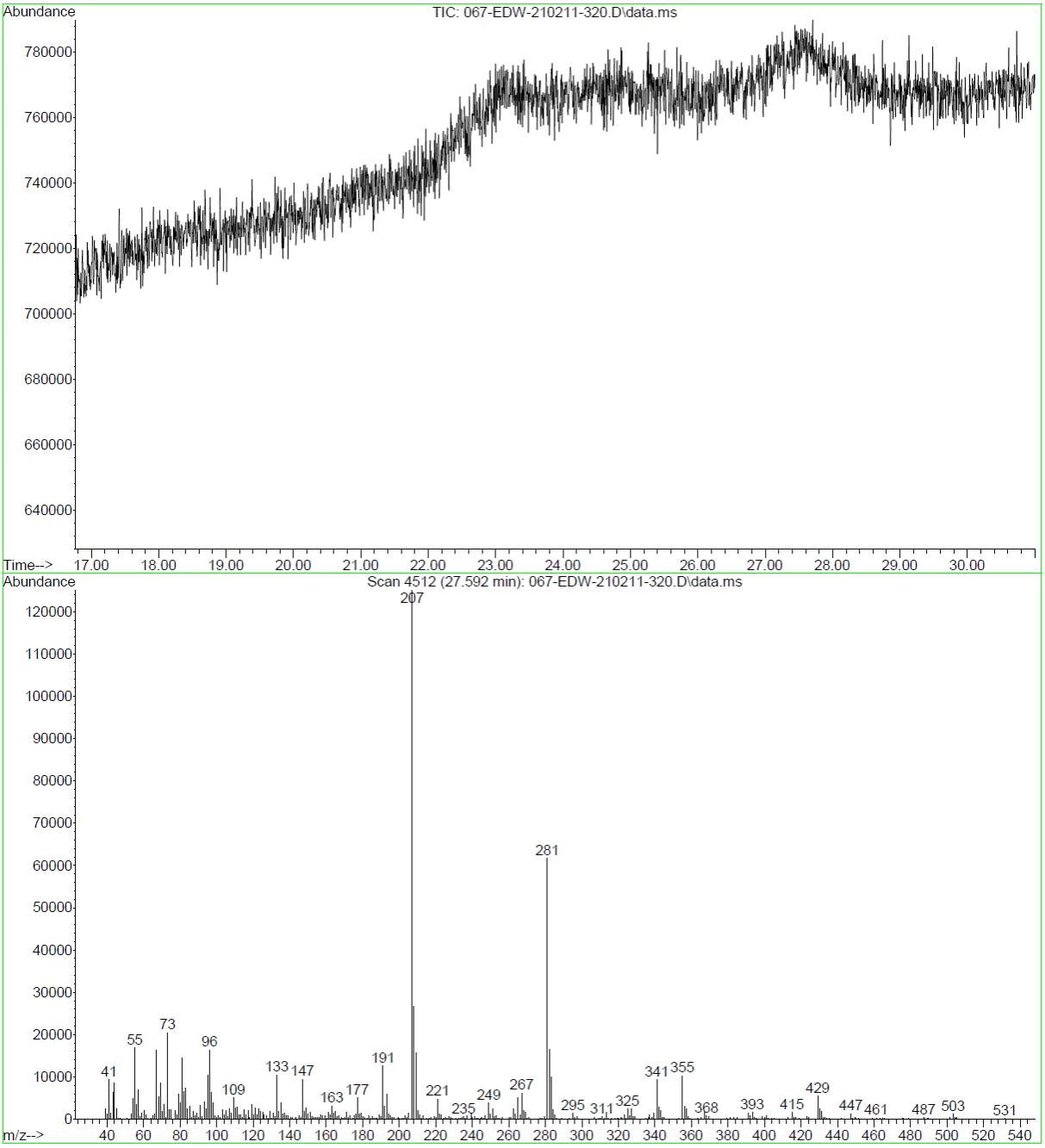

Figure 17. GC-MS chromatogram and mass spectrum performed on an Agilent GC-FID-MS with a DB-1ms column with a ramp rate of 30°C/min and a final oven temperature of 320°C.

Figure 18

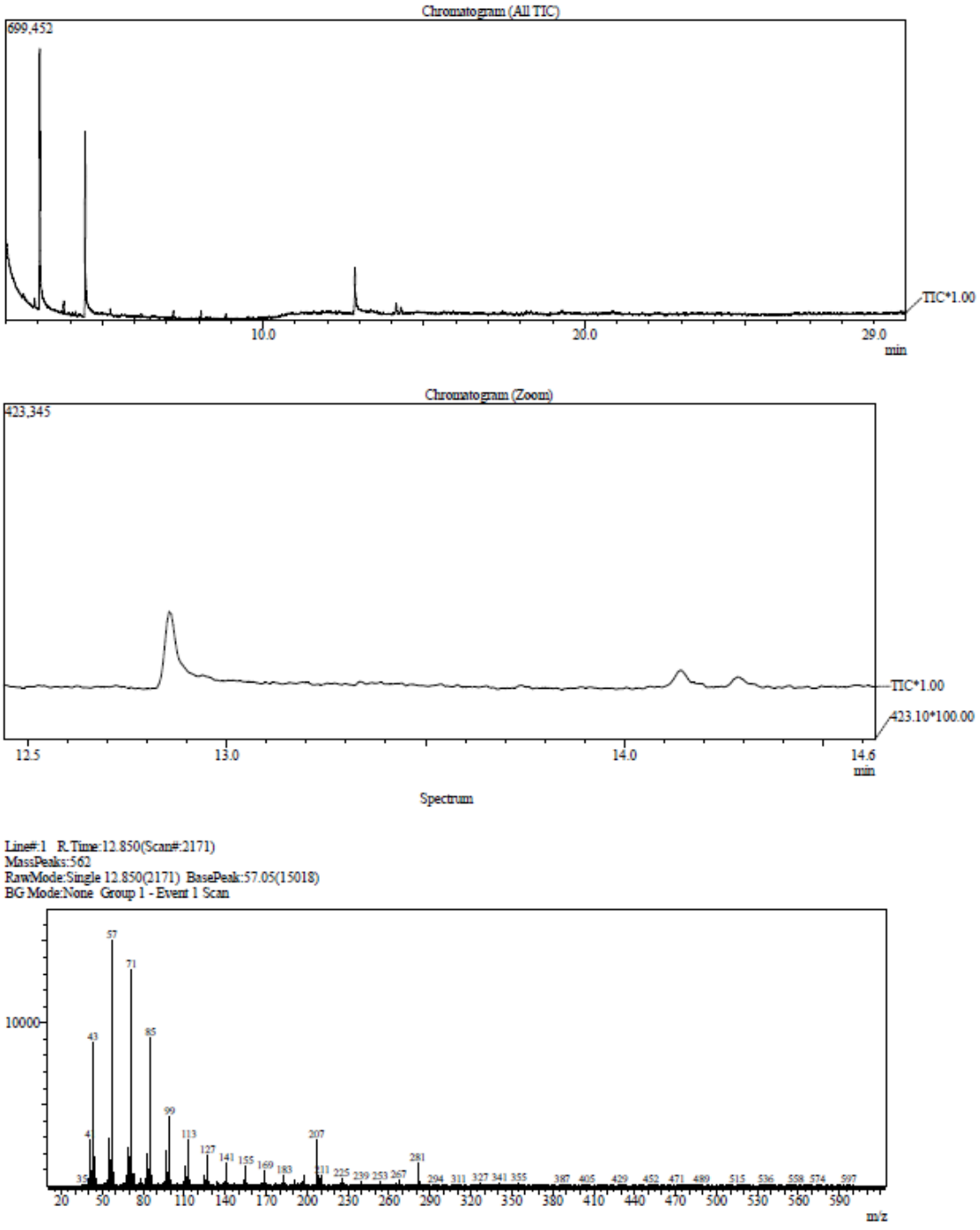

Figure 18. GC-MS chromatogram and mass spectrum at a retention time of 12.850 min using the Shimadzu GC-MS with an RX1-5MS column.

Figure 19

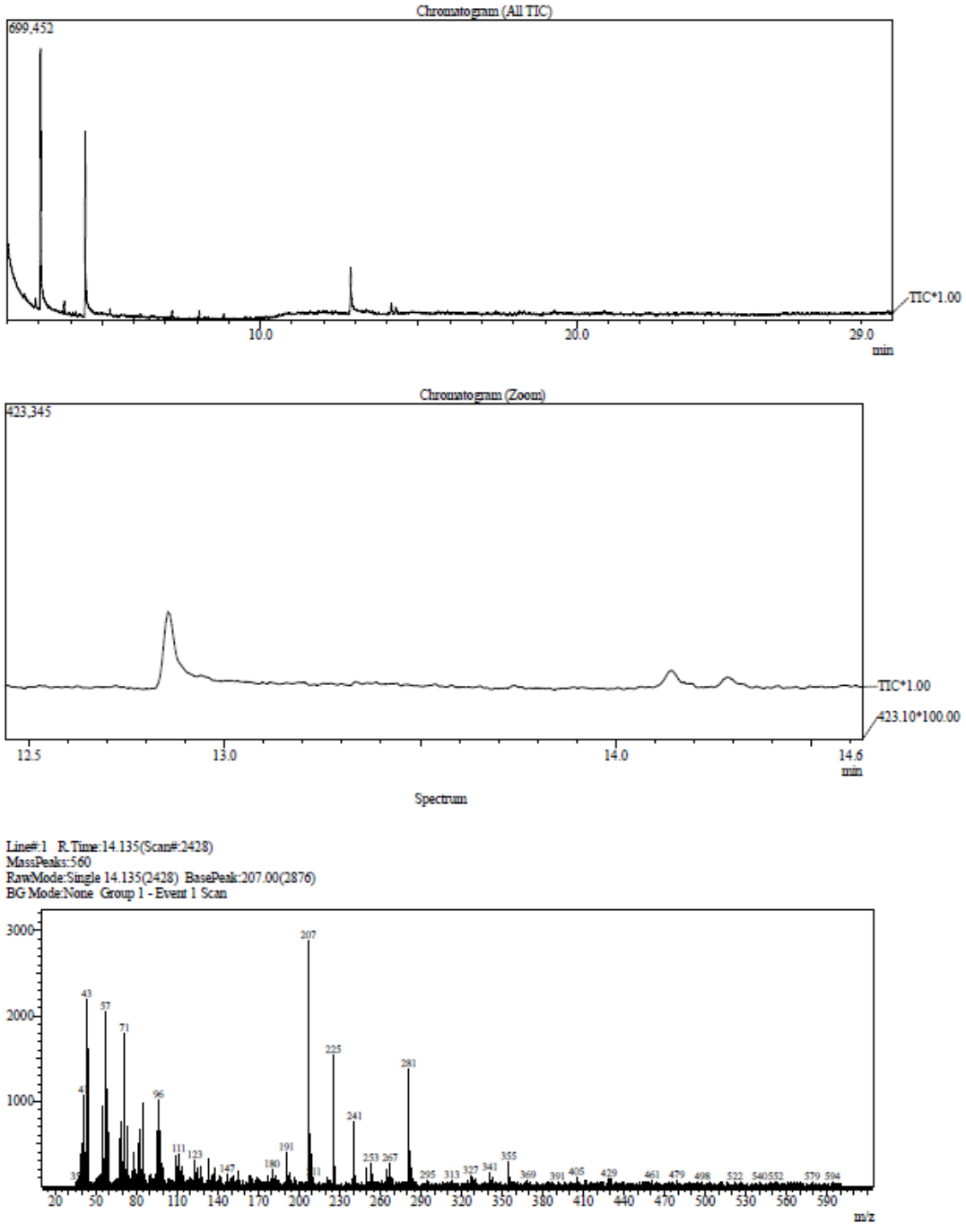

Figure 19. GC-MS chromatogram and mass spectrum at a retention time of 14.135 min using the Shimadzu GC-MS with an RX1-5MS column.

Figure 20

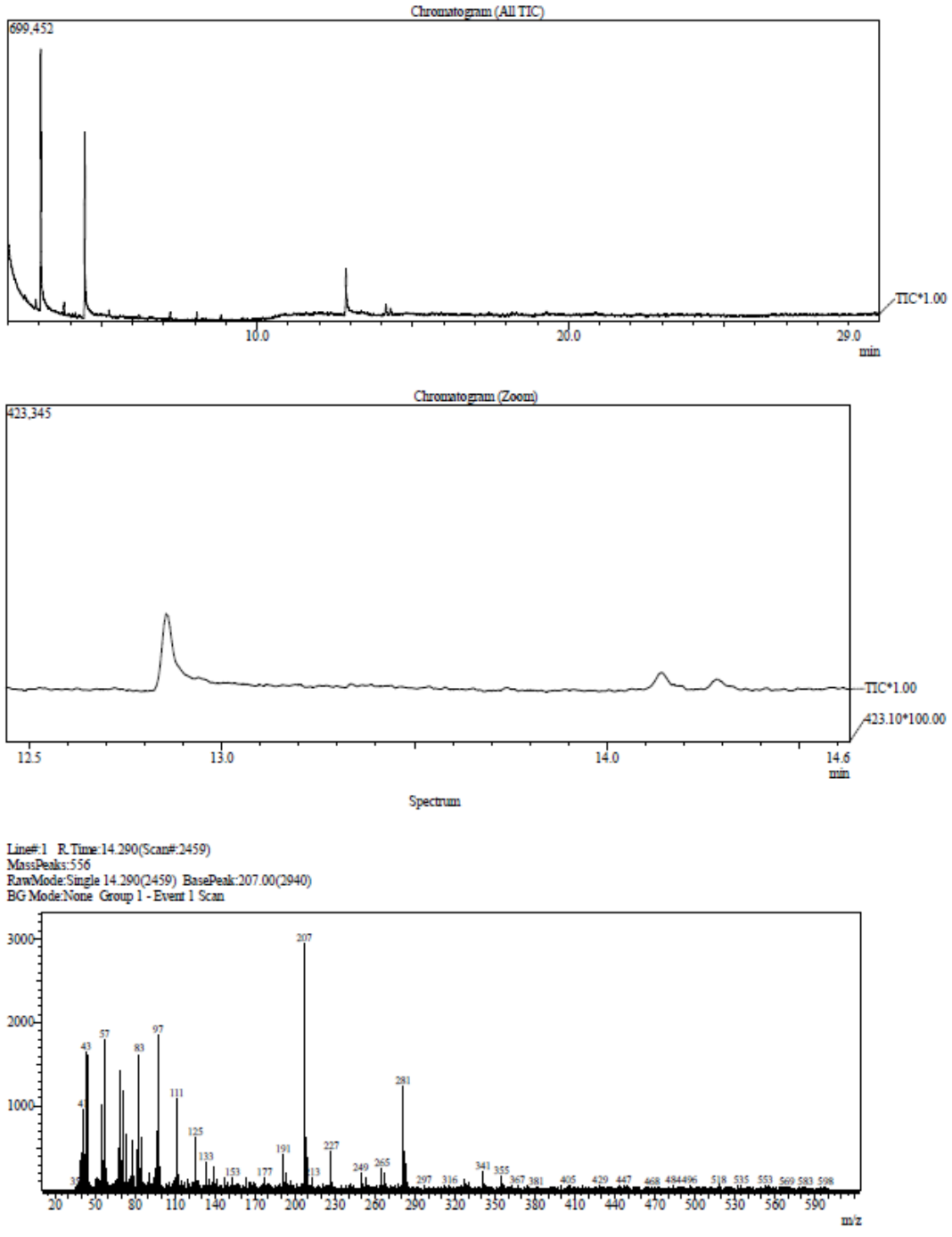

Figure 20. GC-MS chromatogram and mass spectrum at a retention time of 14. 290 min using the Shimadzu GC-MS with an RX1-5MS column.

Figure 21

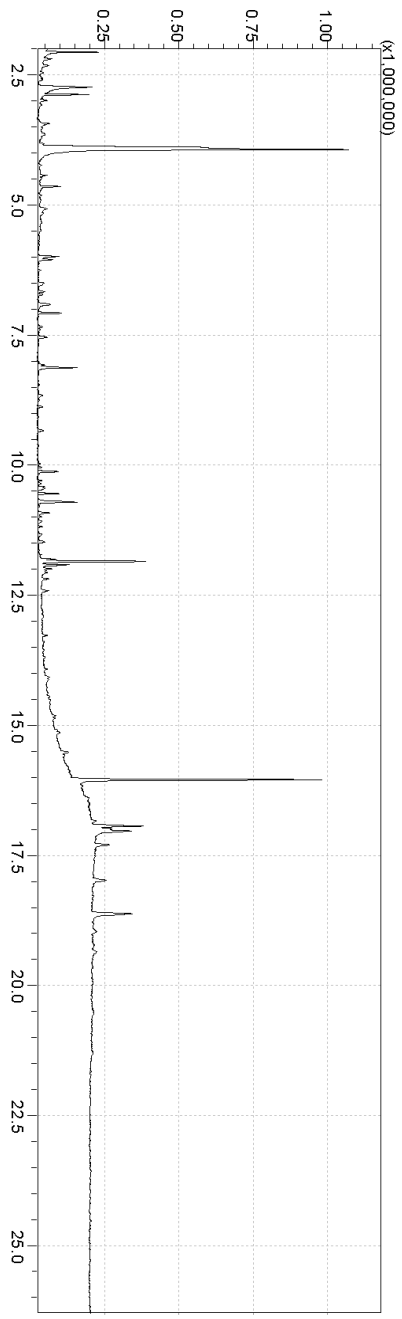

Figure 21. GC-MS chromatogram of kale extract analyzed using a Shimadzu GC-MS with an HP-5ms column.

Figure 22

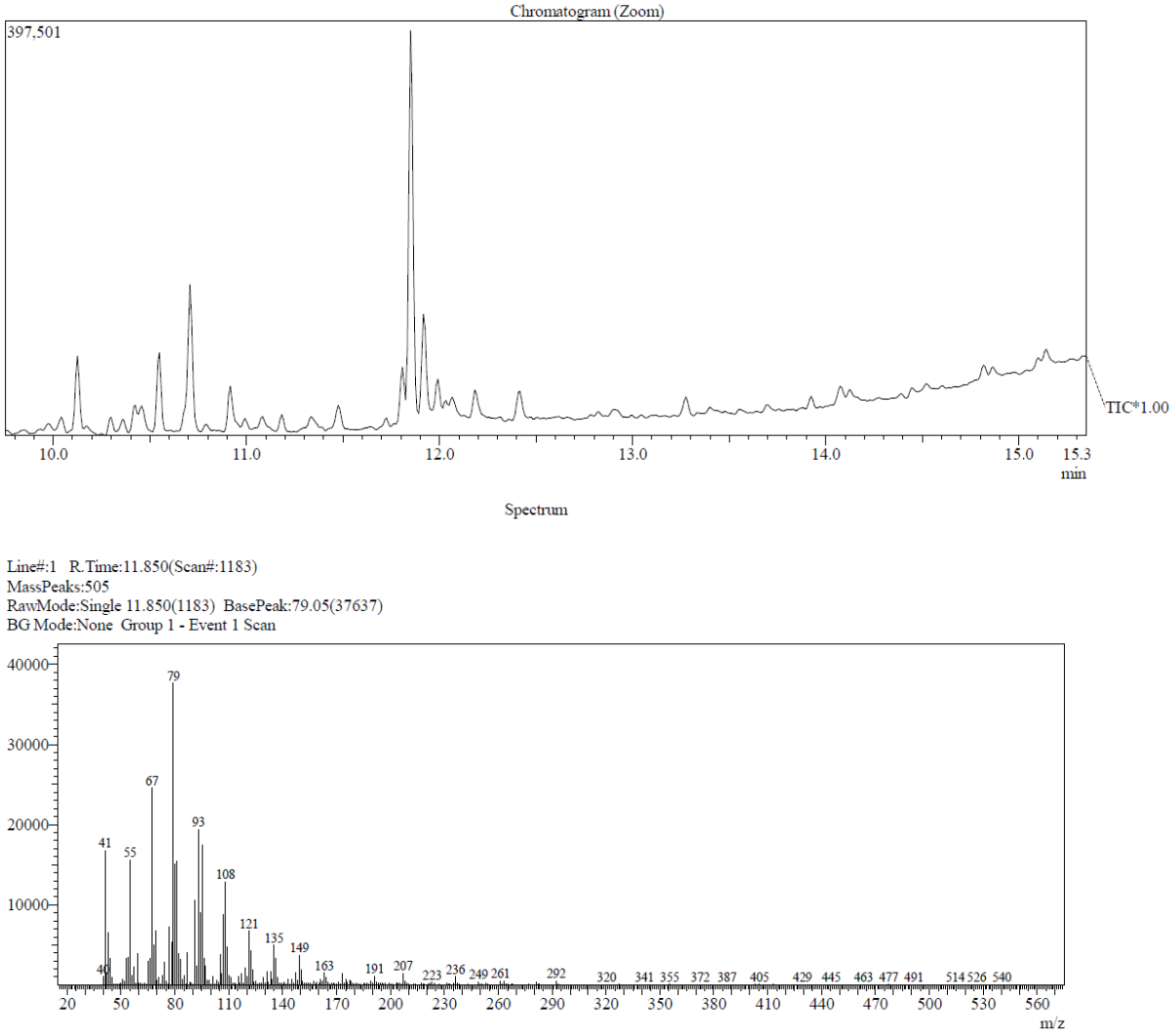

Figure 22. GC-MS chromatogram of kale extract analyzed using a Shimadzu GC-MS with an HP-5ms column with the mass spectrum at a retention time of 11.850 min.

Figure 23

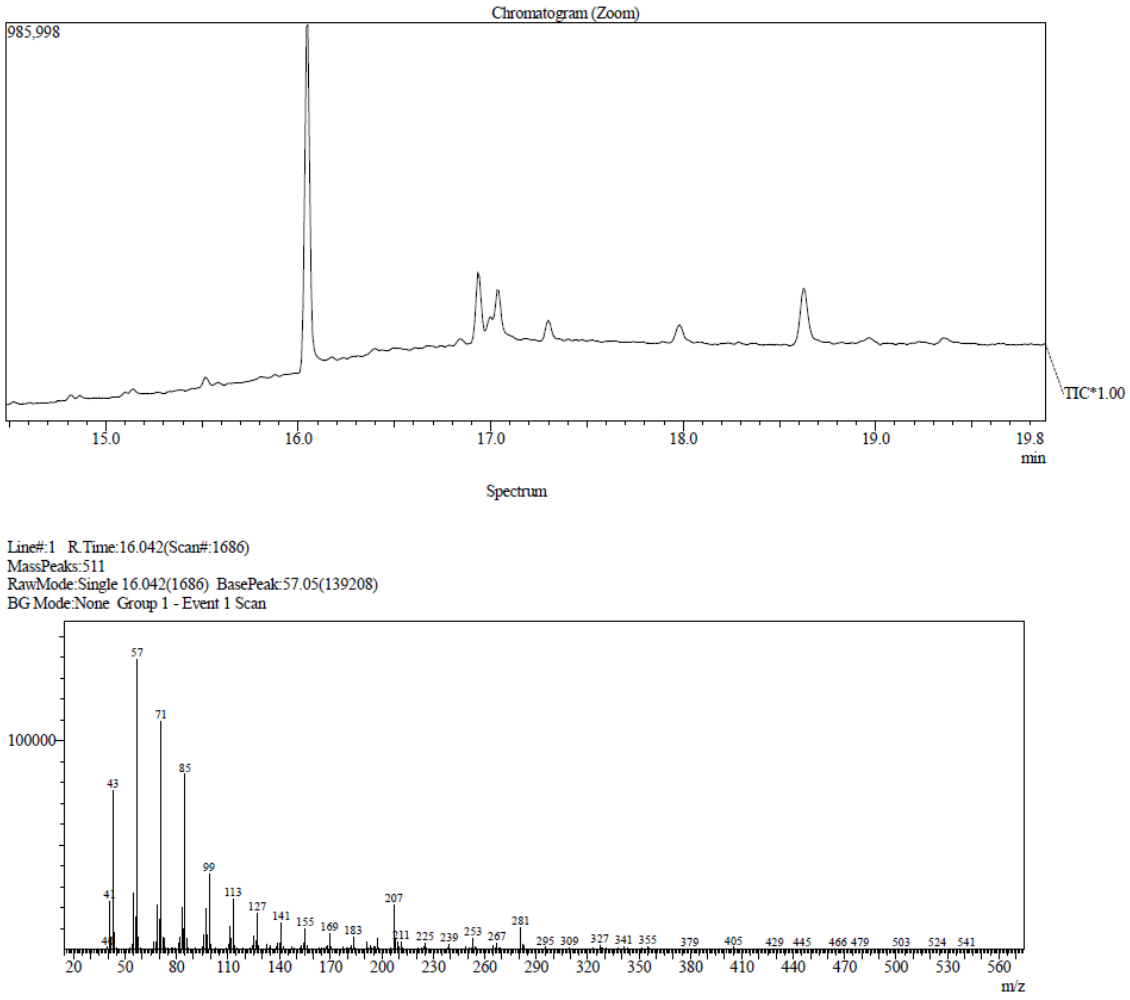

Figure 23. GC-MS chromatogram of kale extract analyzed using a Shimadzu GC-MS with an HP-5ms column with the mass spectrum at a retention time of 16.042 min.

Figure 24

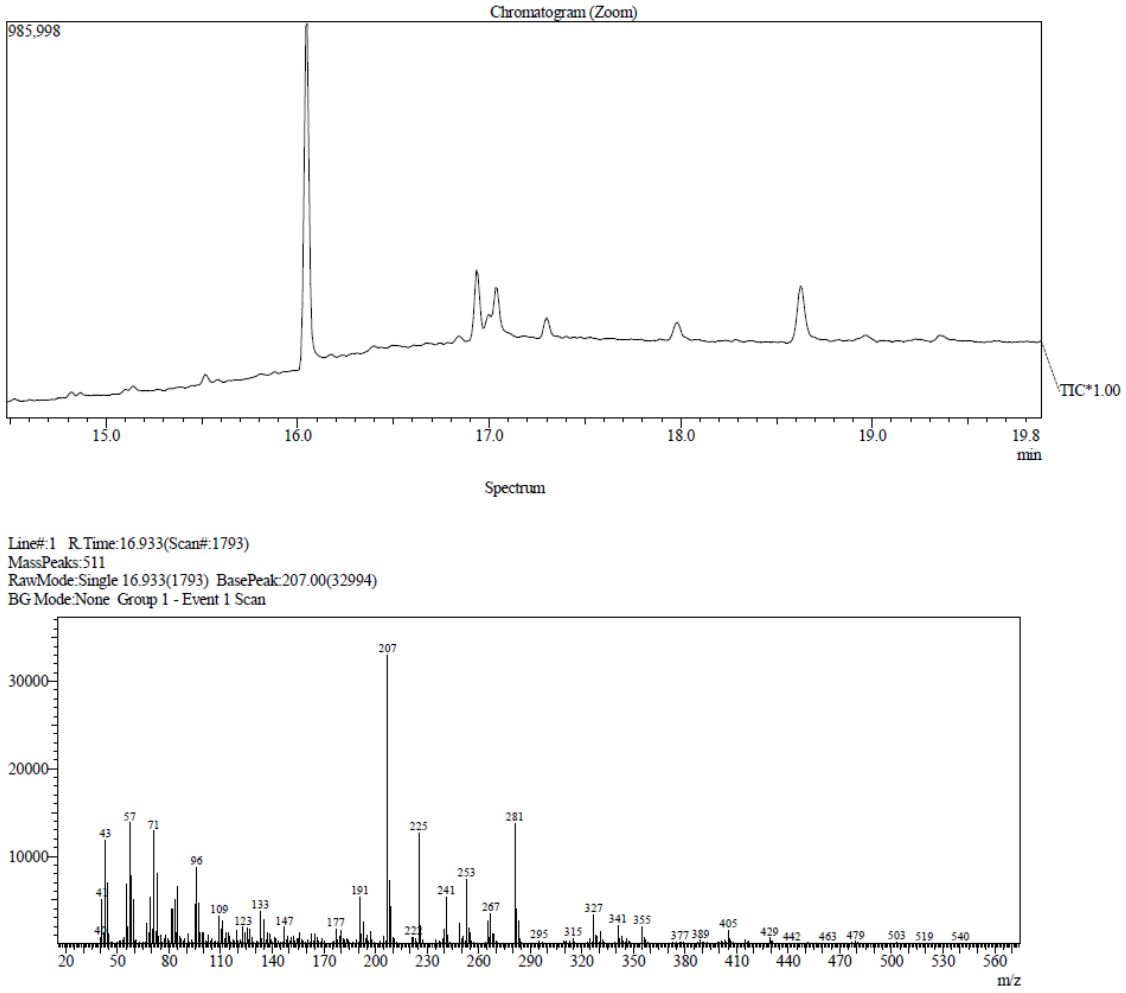

Figure 24. GC-MS chromatogram of kale extract analyzed using a Shimadzu GC-MS with an HP-5ms column with the mass spectrum at a retention time of 16.933 min.

Figure 25

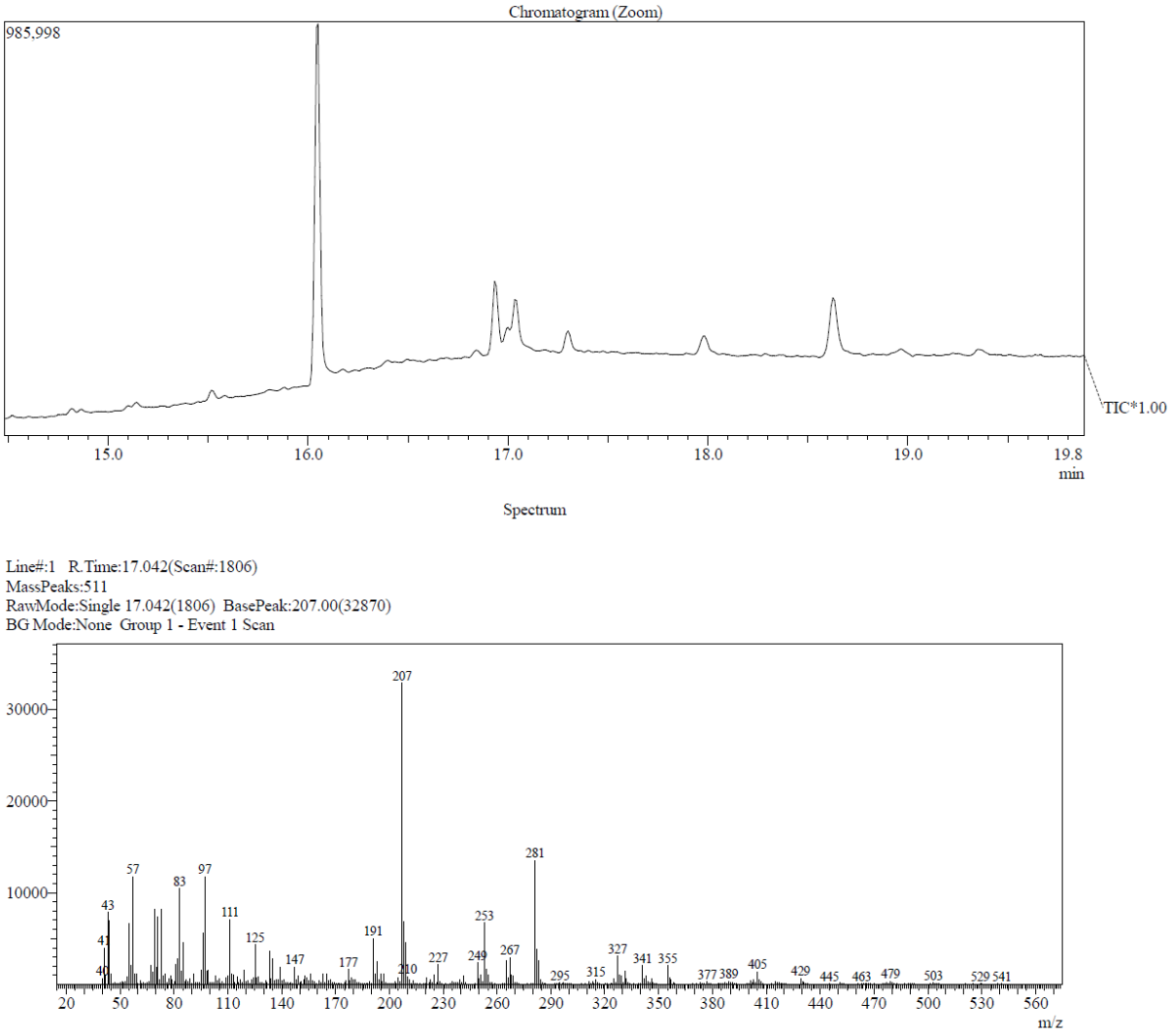

Figure 25. GC-MS chromatogram of kale extract analyzed using a Shimadzu GC-MS with an HP-5ms column with the mass spectrum at a retention time of 17.042 min.

Figure 26

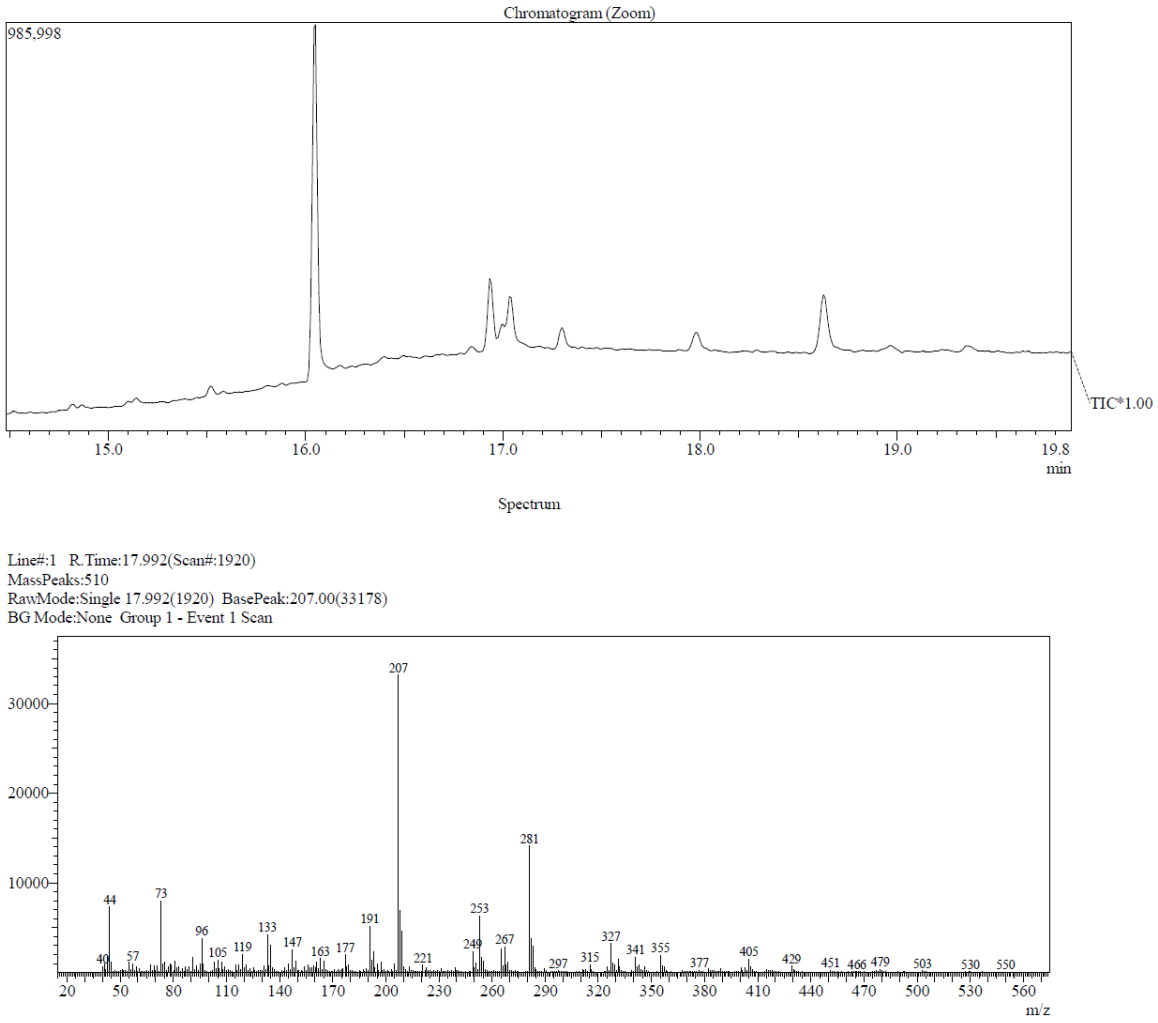

Figure 26. GC-MS chromatogram of kale extract analyzed using a Shimadzu GC-MS with an HP-5ms column with the mass spectrum at a retention time of 17.992 min.

Figure 27

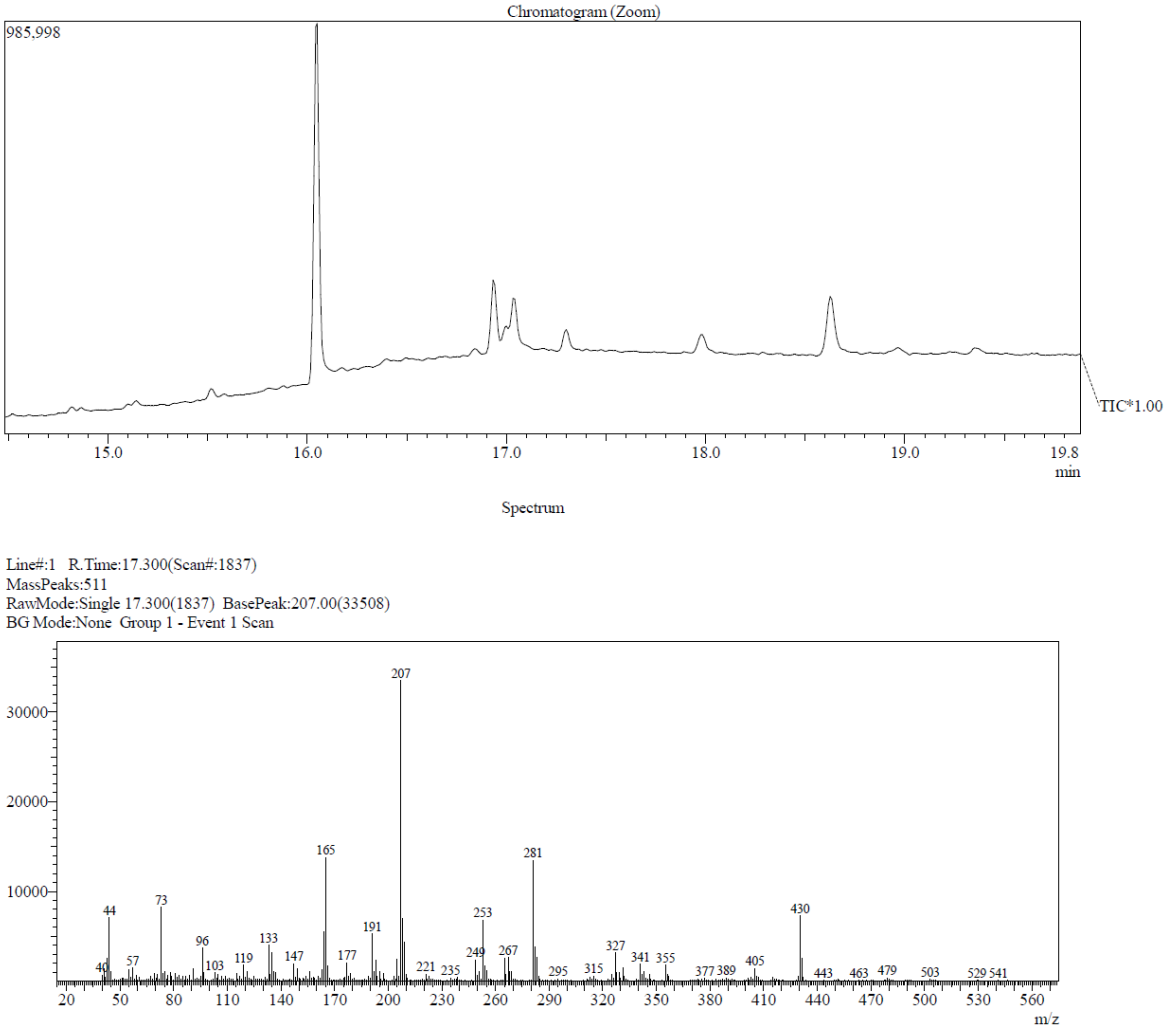

Figure 27. GC-MS chromatogram of kale extract analyzed using a Shimadzu GC-MS with an HP-5ms column with the mass spectrum at a retention time of 17.300 min.

Figure 28

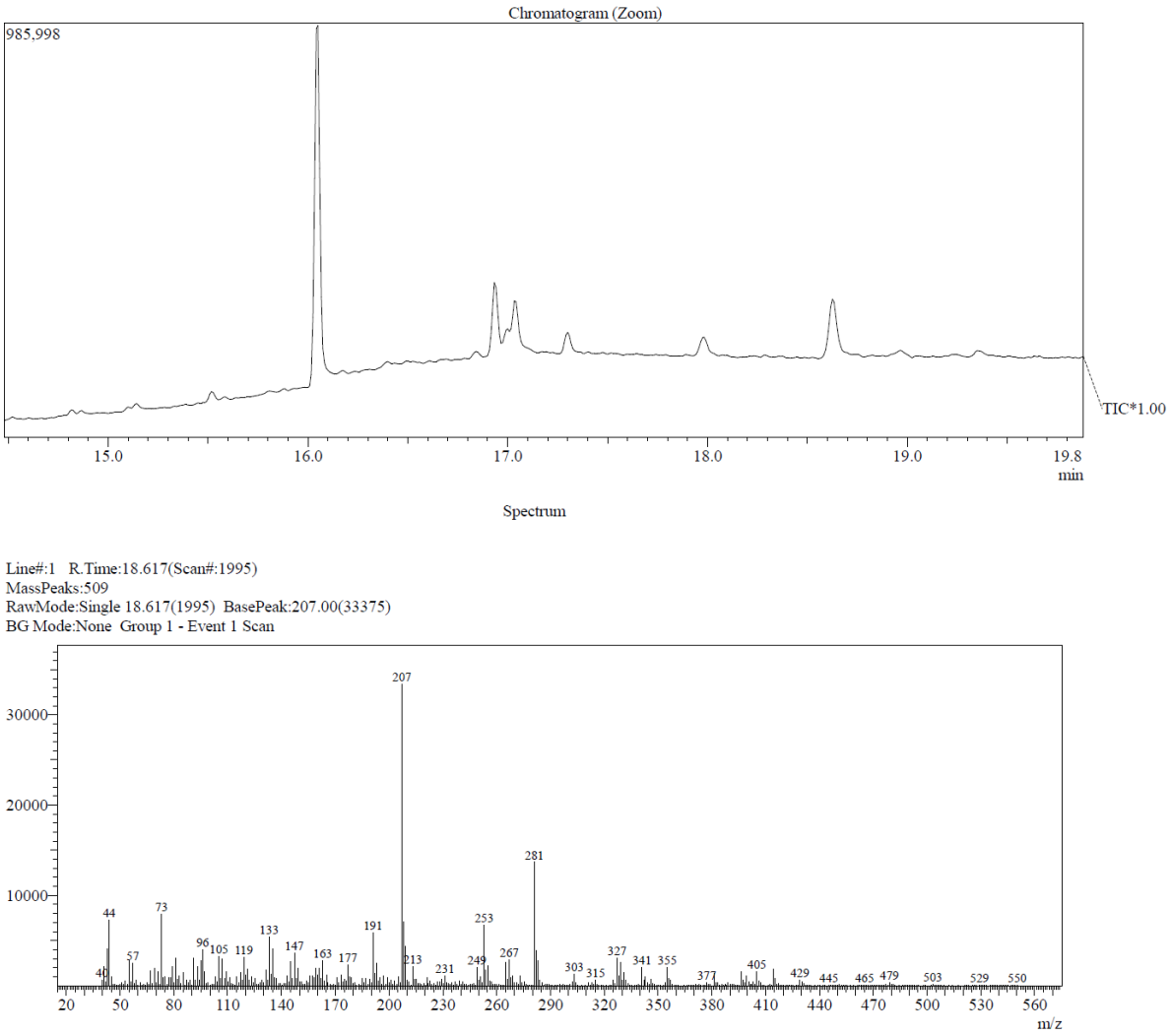

Figure 28. GC-MS chromatogram of kale extract analyzed using a Shimadzu GC-MS with an HP-5ms column with the mass spectrum at a retention time of 18.617 min.

Figure 29

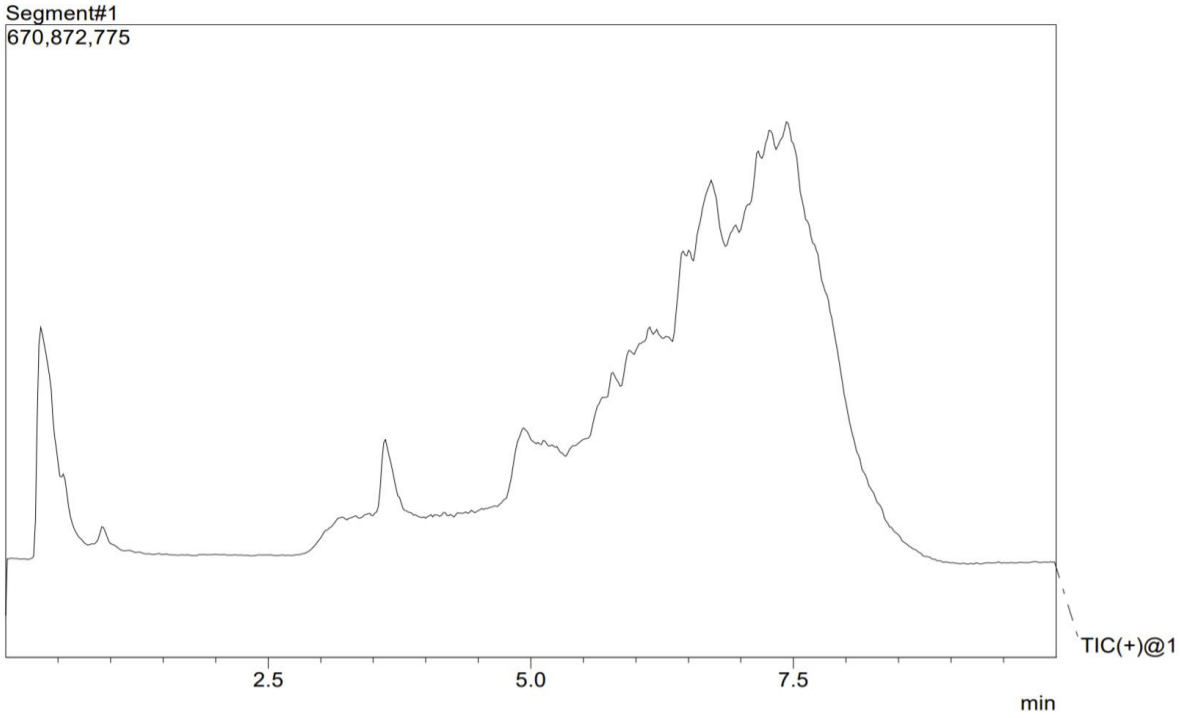

Figure 29. LC-MS/MS total ion chromatogram of kale extract.

Figure 30

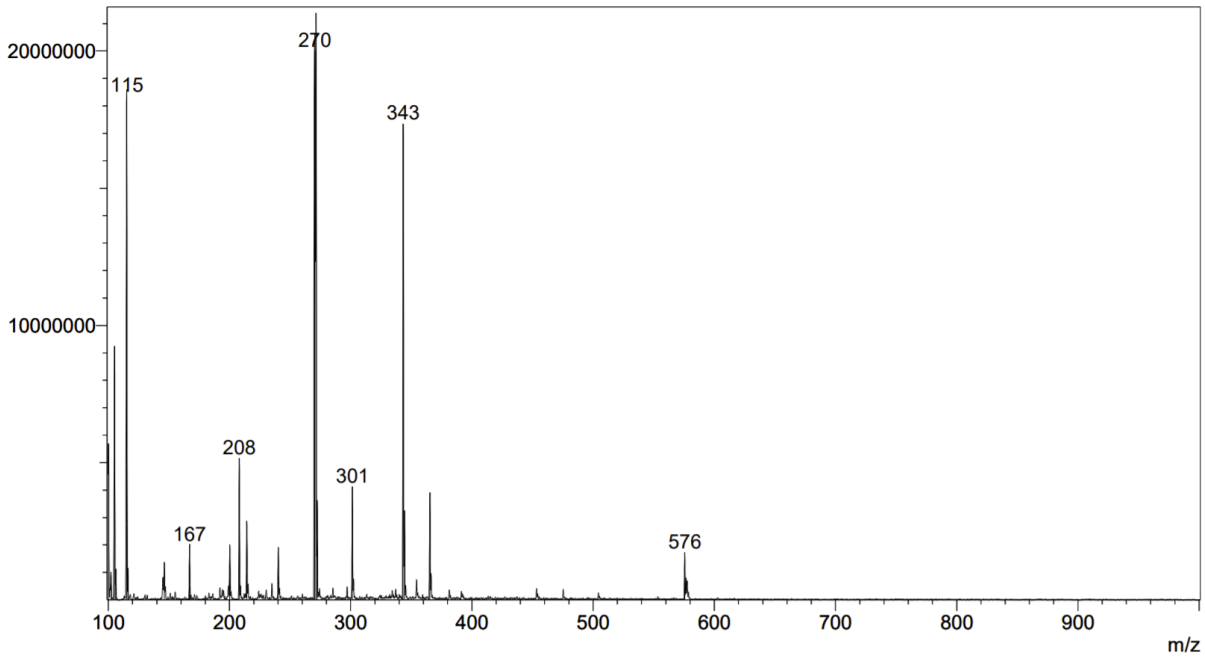

Figure 30. Mass spectrum at a retention time of 4.950 min from LC-MS/MS.

Figure 31

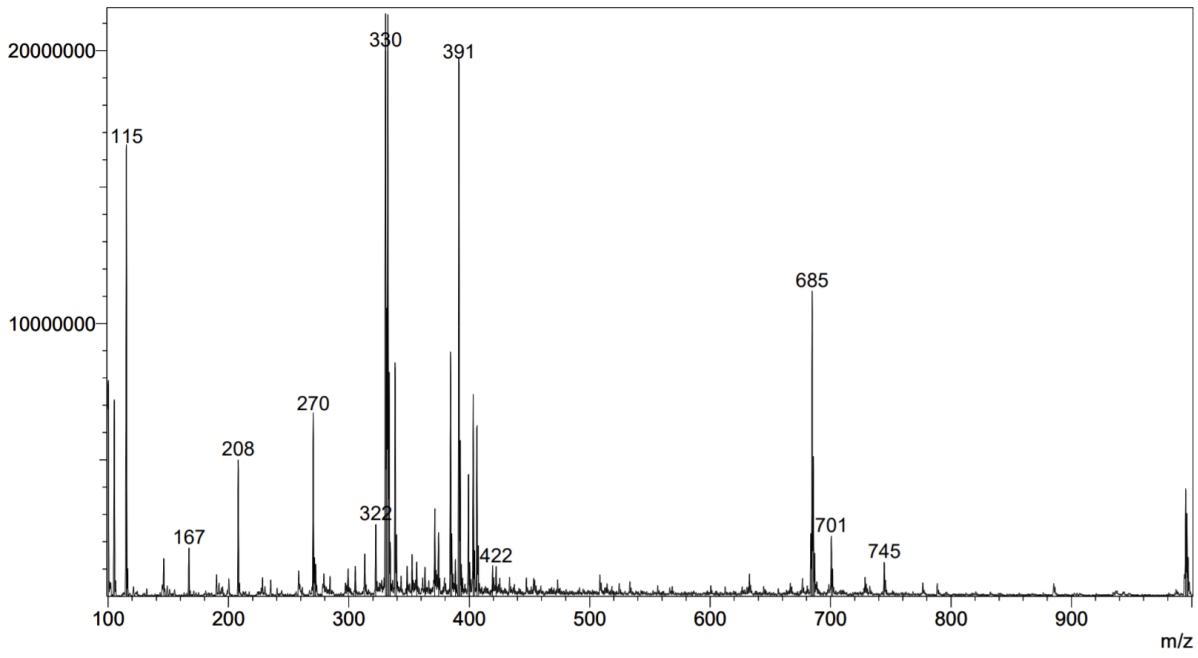

Figure 31. Mass spectrum at a retention time of 6.450 min from LC-MS/MS.

Figure 32

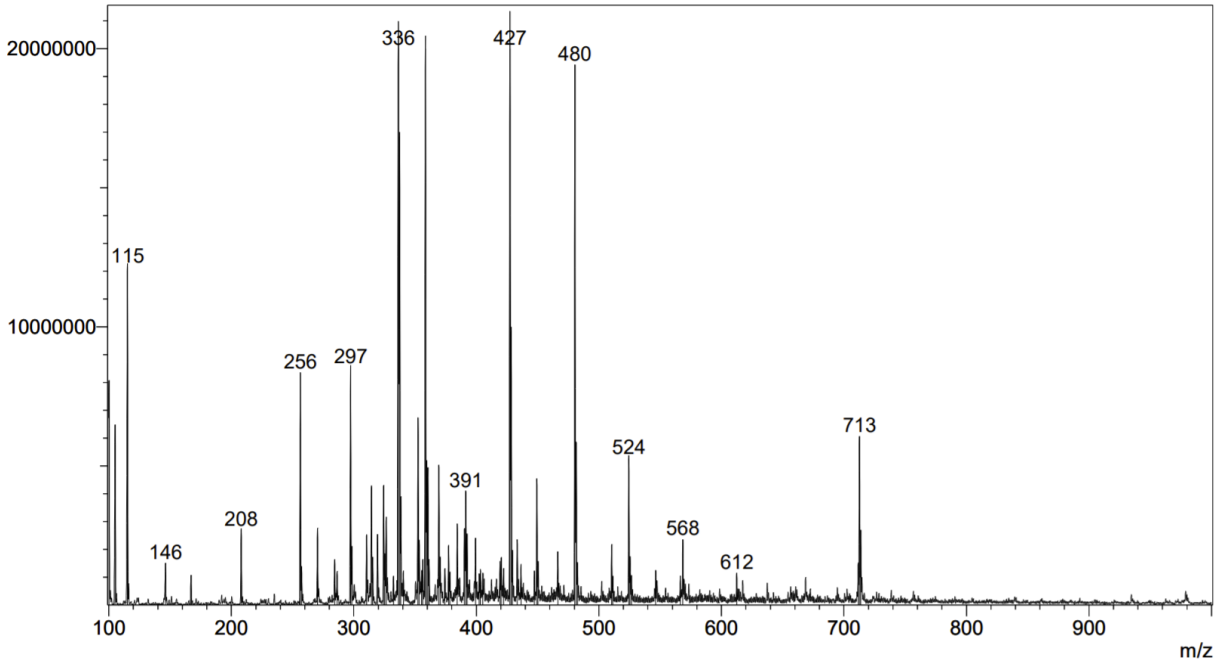

Figure 31. Mass spectrum at a retention time of 7.300 min from LC-MS/MS.

Appendix

Appendix A-Supplementary Figures

A-1

a)

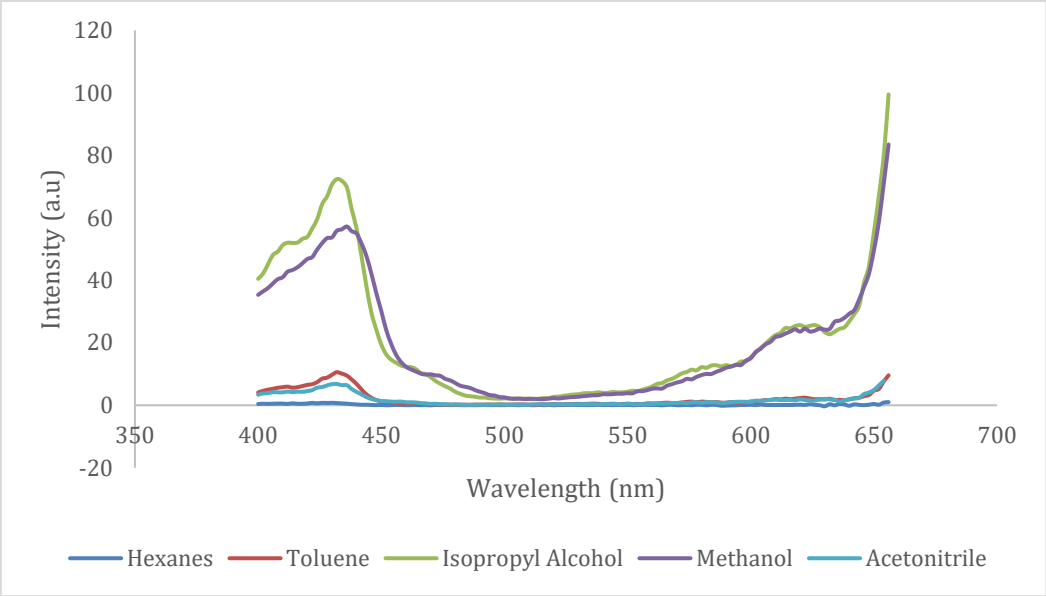

b)

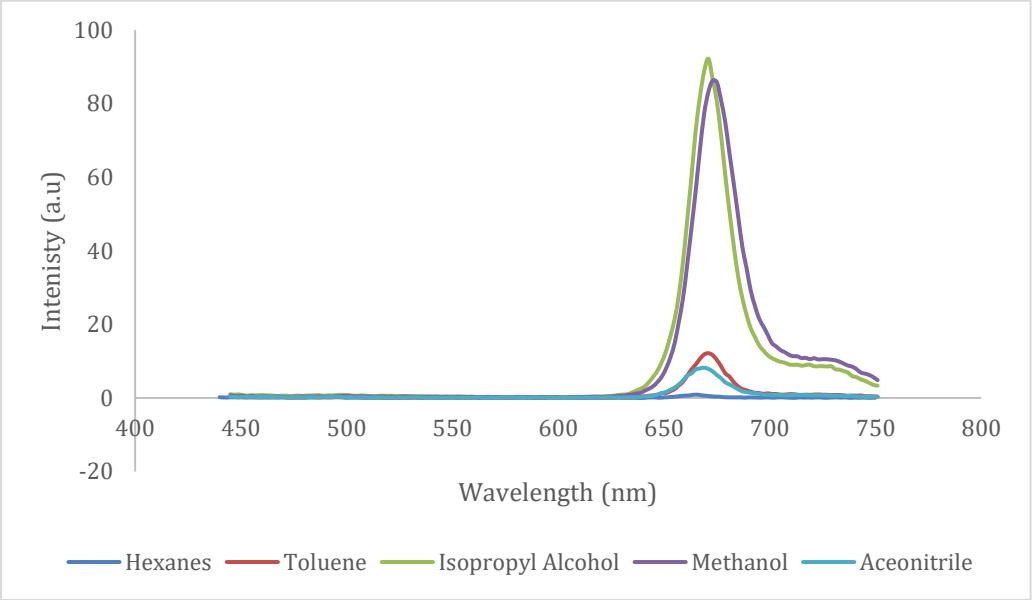

A-1. a) Excitation scan of extracts in different solvents with an emission of ~670 nm. b) Emission scan of extracts in different solvents with an excitation of ~430 nm.

A-2

a)

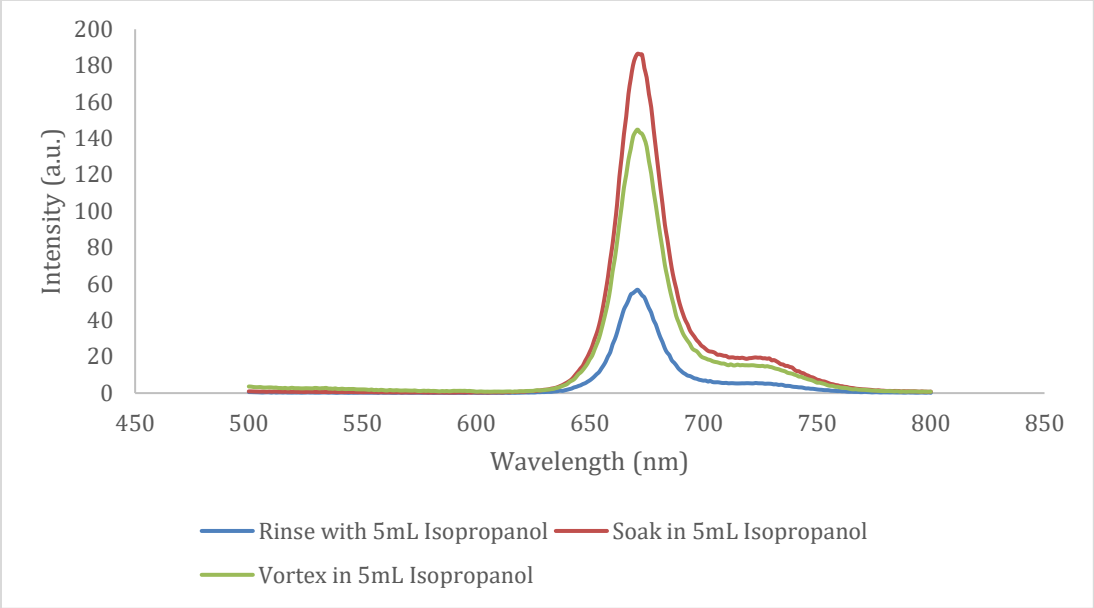

b)

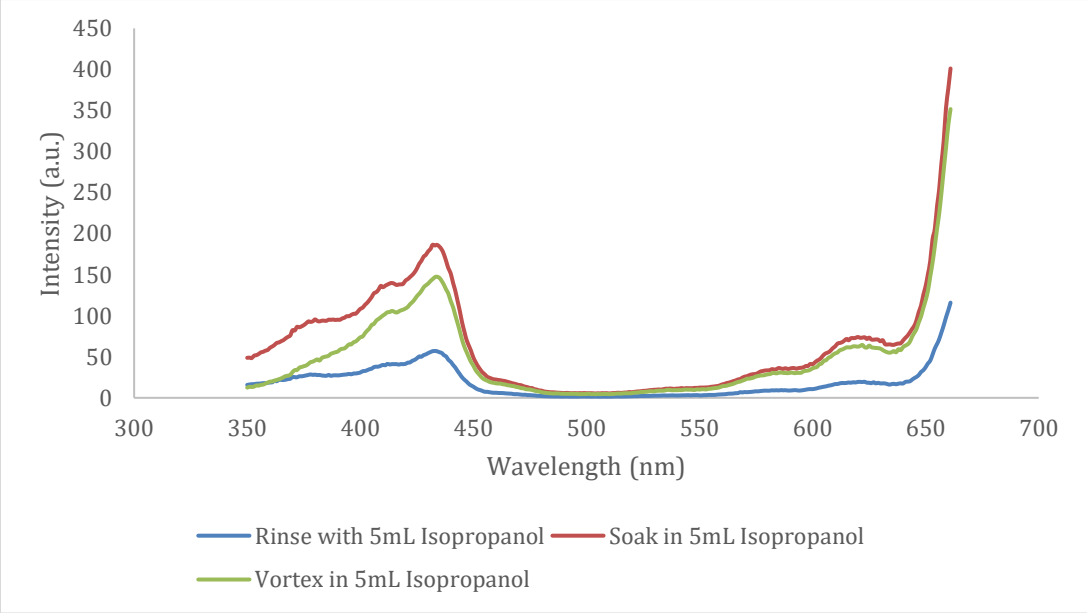

A-2. a) Comparison of emission scans from kale extracts using different extraction techniques with an excitation wavelength of 435 nm. b) Comparison of excitation scans from kale extracts using different extraction techniques with emission wavelengths of 661 nm - 671 nm.

Appendix B-Chemical Structures

B-1

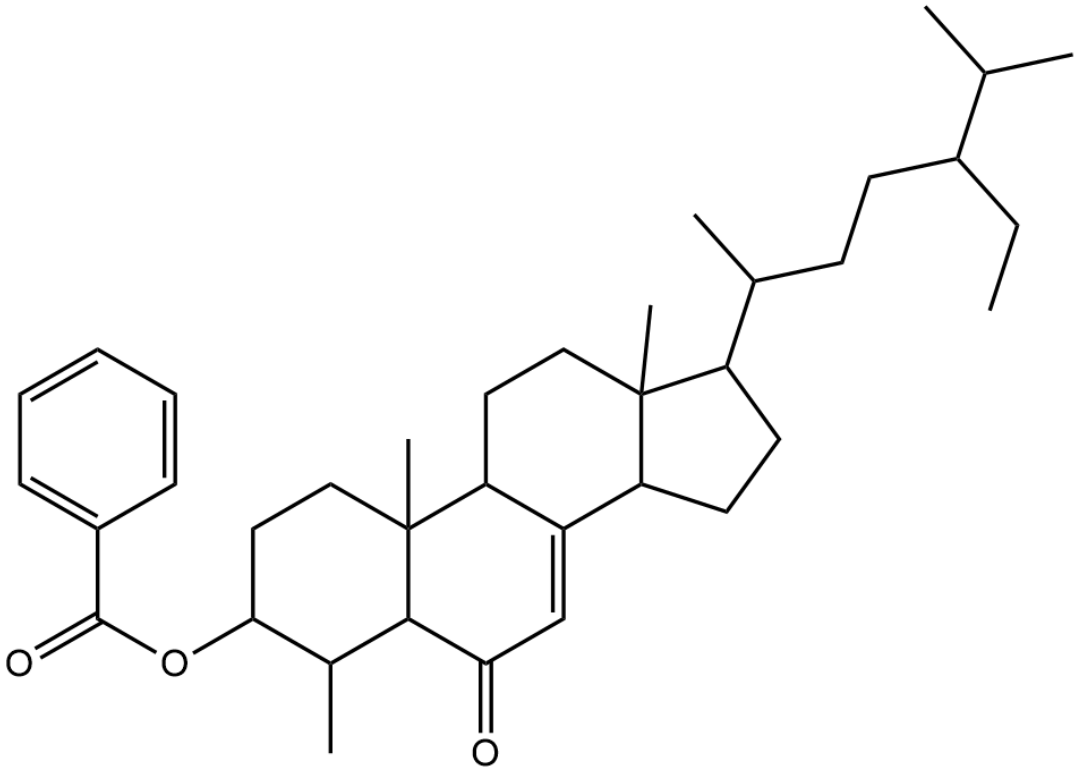

B-1. Chemical structure of 22-desoxycarpesterol (PubChem Compound Summary for CID 537200, Deoxycarpesterol, 2021).

B-2

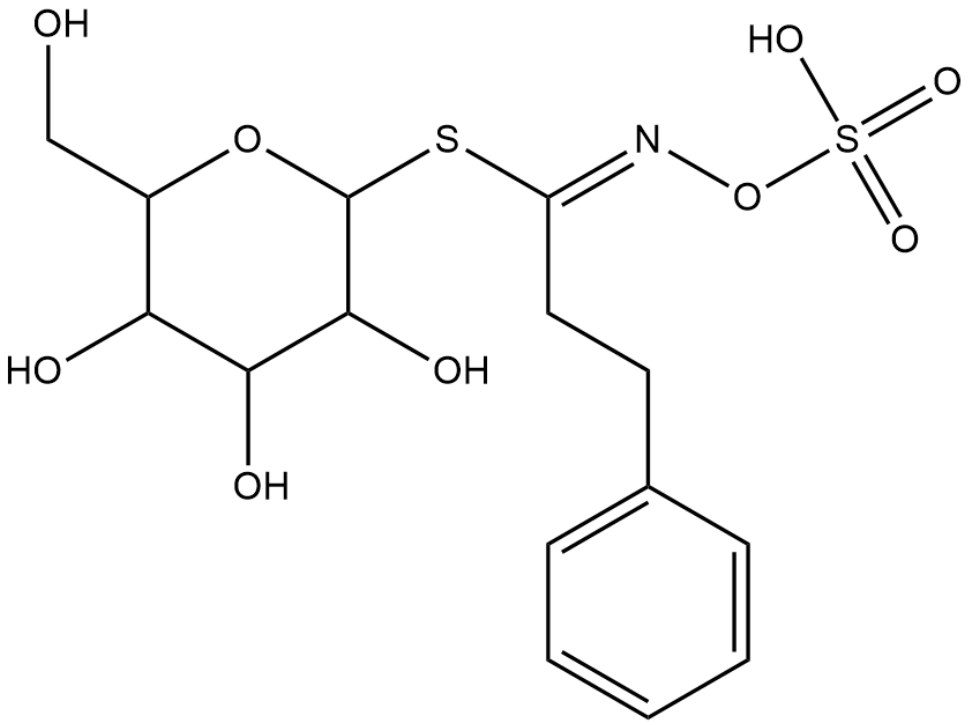

B-2. Chemical structure of Gluconasturtiin (Gluconasturtiin, 2020).

B-3

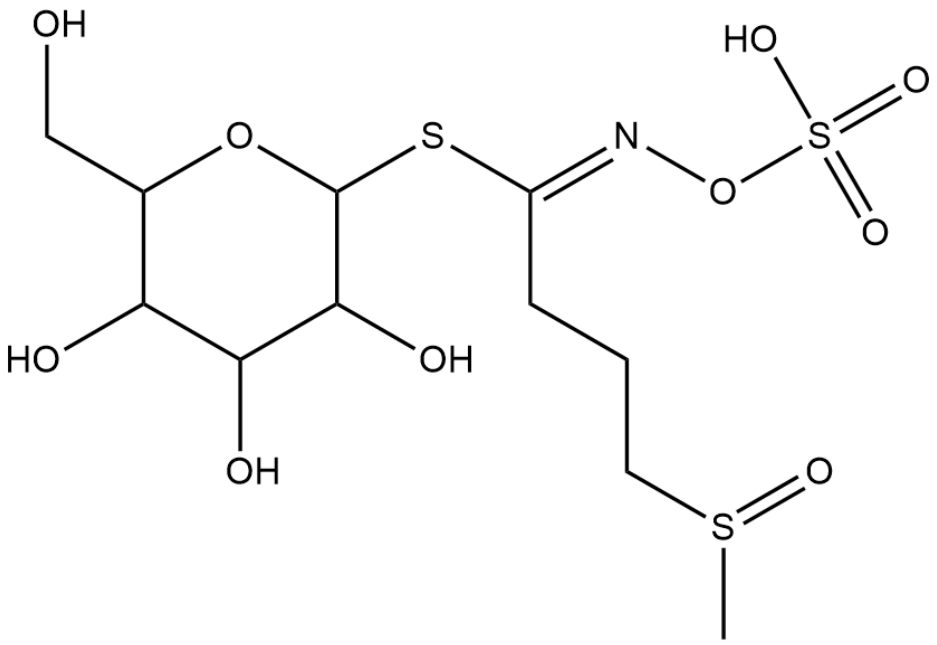

B-3. Chemical structure of Gluoiberin (PubChem Compound Summary for CID 6602303, Glucoiberin, 2021).

B-4

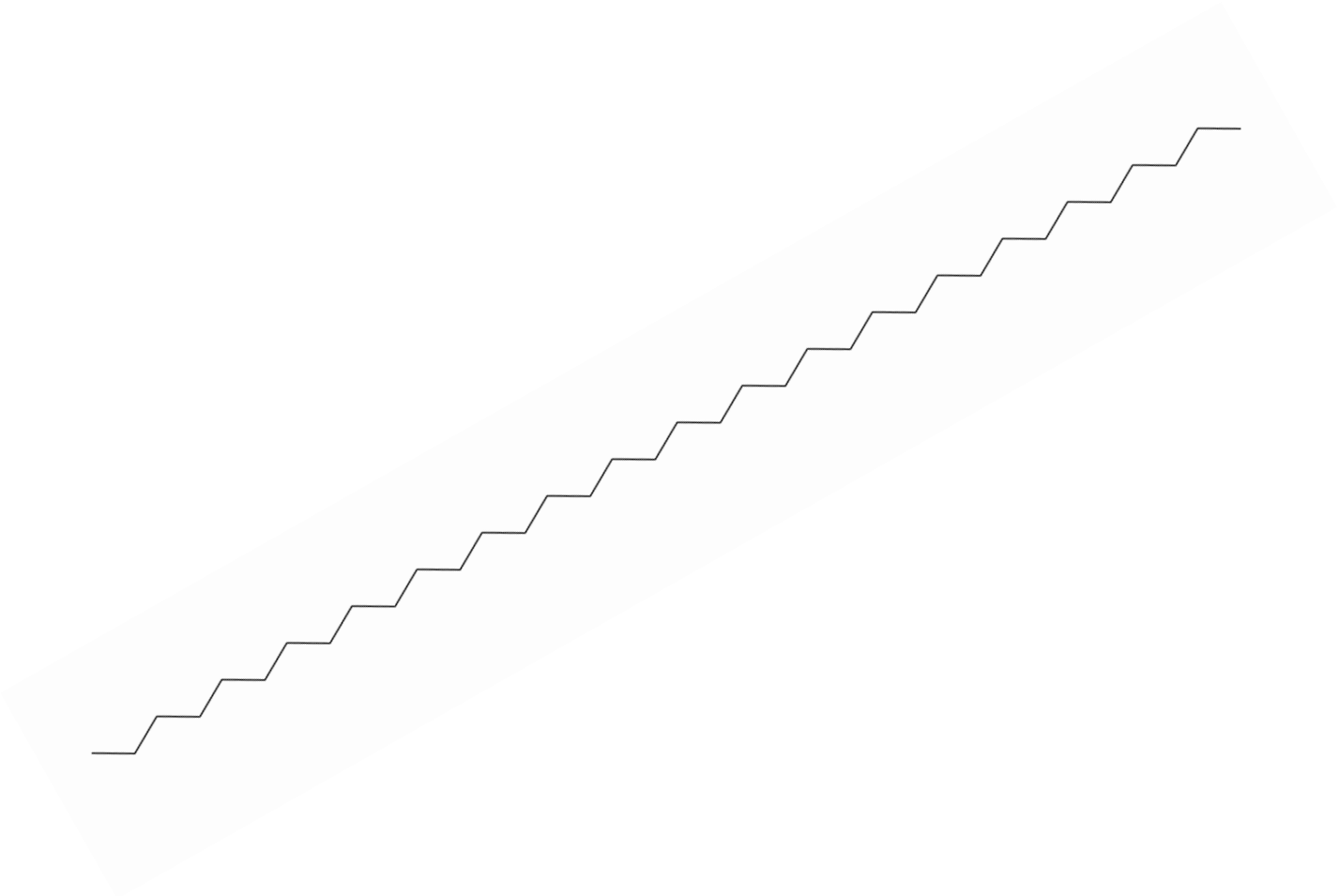

B-4. Chemical structure of Hexatriacontane (PubChem Compound Summary for CID 12412, Hexatriacontane, 2021).

B-5

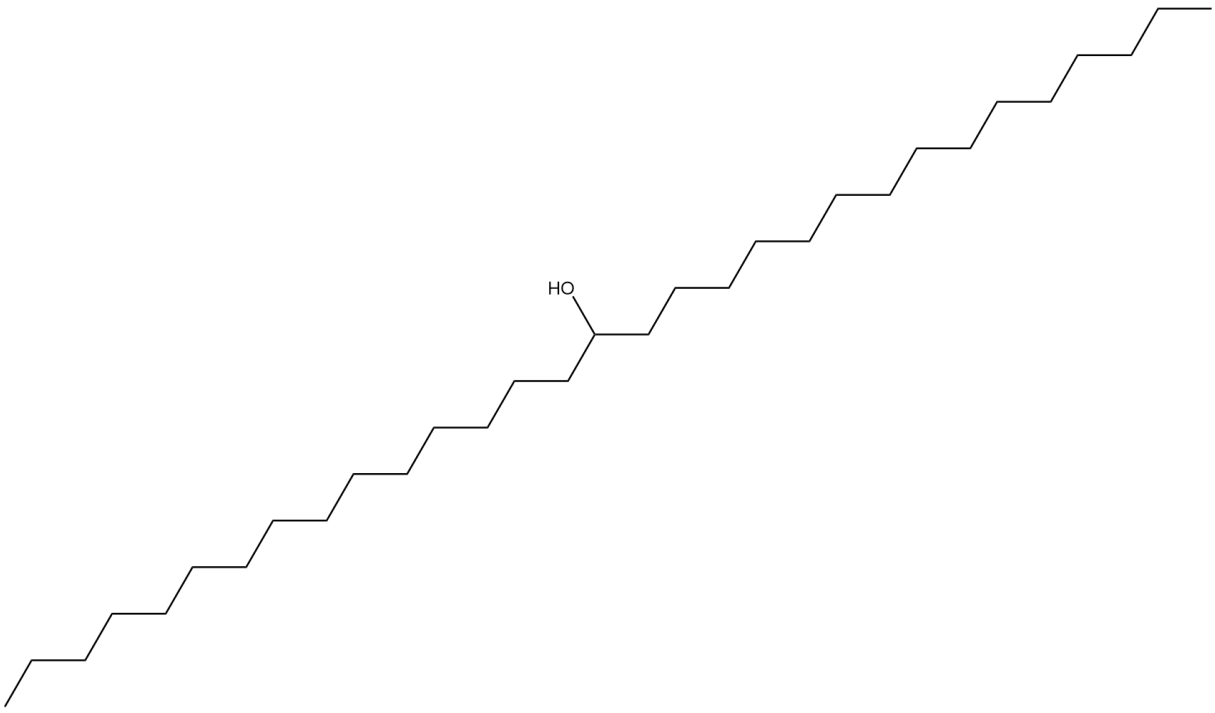

B-5. Chemical structure of 16-Hentriaconanol (PubChem Compound Summary for CID 9548843, Hentriacontan-16-ol, 2021)

B-6

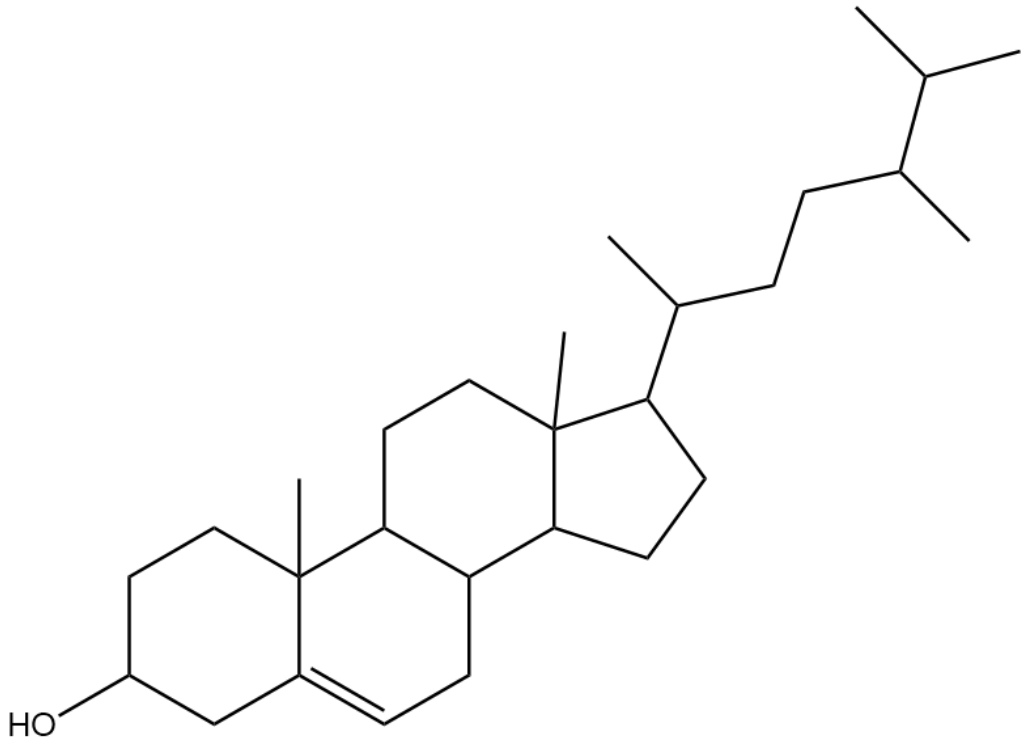

B-6. Chemical structure of campesterol (PubChem Compound Summary for CID 173183, Campesterol, 2021).

B-7

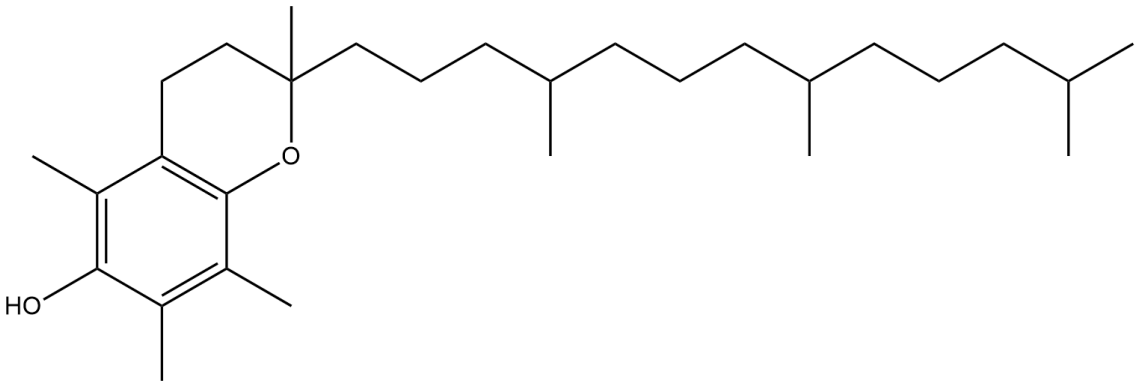

B-7. Chemical structure of alpha-Tocopherol (PubChem Compound Summary for CID 1742129, (-)-alpha-Tocopherol, 2021).

B-8

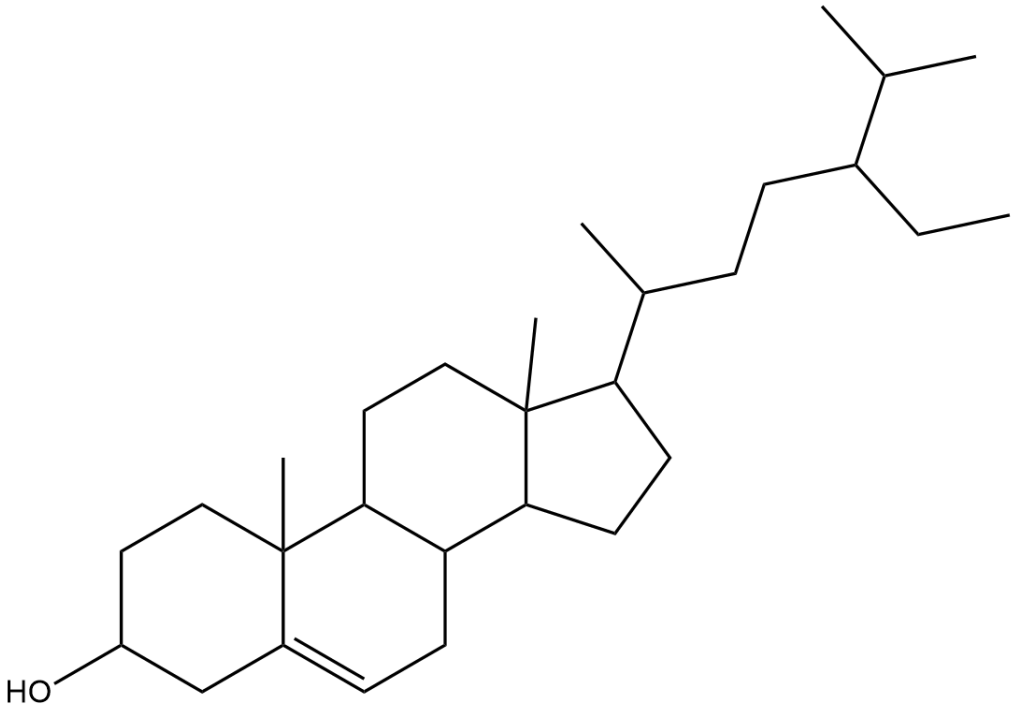

B-8. Chemical structure of gamma-Sitosterol (PubChem Compound Summary for CID 133082557, gamma-Sitosterol monohydrate, 2021).

Vita

Elora Wall was born and raised in New Orleans, Louisiana. She attended the oldest continuously operating all-girl Catholic school in the United States, Ursuline Academy, from pre-kindergarten to twelfth grade. In May 2017, she graduated from the Roger Hadfield Ogden Honors College at Louisiana State University where she earned Bachelor of Science degrees in Chemistry, Biochemistry, and Biological Sciences. She successfully defended her undergraduate Honors Research Thesis entitled “Synthesis of β-Methyl-L-Cysteine as a Model for a β-Methyl-D-Cysteine Building Block for Incorporation into Microbisporicins” under the direction of Dr. Carol Taylor. She has also presented posters at both the Southwest Regional Meeting of the American Chemical Society and the American Academy of Forensic Sciences Annual Scientific Meeting. She will graduate with her Master of Forensic Science with a concentration of Forensic Chemistry/Trace in May 2021.

References

Agilent Technologies. (n.d.). *What are the common contaminants in my GCMS.* Retrieved from Agilent Technologies: https://www.agilent.com/cs/library/Support/Documents/FAQ232%20F05001.pdf

Consortium, M. (2021). *MassBank High Quality Spectral Database*. Retrieved from MassBank: https://massbank.eu/MassBank/

Cristina E. Stanciu, e. a. (2016). Analysis of Red Autofluorescence (650-670nm) in Epidermal Cell Populations and Its Potential for Distinguishing Contributors to 'Touch' Biological Samples. *F1000Research, 5*, 18.

Executive Office of the President President's Council of Advisors on Science and Technology. (2016). *Report to the President Forensic Science in Criminal Courts: Ensuring Scientific Validity of Feature-Comparison Methods.* Retrieved from https://obamawhitehouse.archives.gov/sites/default/files/microsites/ostp/PCAST/pcast_forensic_science_report_final.pdf

Gluconasturtiin. (2020, January 2). Retrieved from Wikipedia The Free Encyclopedia: https://en.wikipedia.org/wiki/Gluconasturtiin

Iva Pavlović, I. P.-S. (2018). Correlations between Phytohormones and Drought Tolerance in Selected Brassica Crops: Chinese Cabbage, White Cabbage and Kale. *International Journal of Molecular Sciences, 19*(10), 2866.

Katherine Philpott, M. e. (2017). Analysis of Cellular Autofluorescence in Touch Samples by Flow Cytometry: Implications for Front End Separation of Trace Mixture Evidence. *Analytical and Bioanalytical Chemistry, 409*(17), 4167–4179.

Marek Haftek, e. a. (1986). Flow Cytometry for Separation of Keratinocyte Subpopulations from the Viable Epidermis. *Journal of Investigative Dermatology, 87*(4), 480–484.

PubChem Compound Summary for CID 12412, Hexatriacontane. (2021). Retrieved April 13, 2021, from National Center for Biotechnology Information: https://pubchem.ncbi.nlm.nih.gov/compound/HEXATRIACONTANE#section=Structures

PubChem Compound Summary for CID 133082557, gamma-Sitosterol monohydrate. (2021). Retrieved April 13, 2021, from National Center for Biotechnology Information: https://pubchem.ncbi.nlm.nih.gov/compound/gamma-Sitosterol-monohydrate

PubChem Compound Summary for CID 173183, Campesterol. (2021). Retrieved April 16, 2021, from National Center for Biotechnology Information: https://pubchem.ncbi.nlm.nih.gov/compound/Campesterol

PubChem Compound Summary for CID 1742129, (-)-alpha-Tocopherol. (2021). Retrieved April 13, 2021, from National Center for Biotechnology Information: https://pubchem.ncbi.nlm.nih.gov/compound/alpha-Tocopherol

PubChem Compound Summary for CID 537200, Deoxycarpesterol. (2021). Retrieved April 21, 2021, from National Center for Biotechnology Information: https://pubchem.ncbi.nlm.nih.gov/compound/Deoxycarpesterol.

PubChem Compound Summary for CID 6602303, Glucoiberin. (2021). Retrieved April 11, 2021, from National Center for Biotechnology Information: https://pubchem.ncbi.nlm.nih.gov/compound/Glucoiberin

PubChem Compound Summary for CID 9548843, Hentriacontan-16-ol. (2021). Retrieved April 16, 2021, from National Center for Biotechnology Information: https://pubchem.ncbi.nlm.nih.gov/compound/Hentriacontan-16-ol

Rahman, A.-u. (Ed.). (2014). *Studies in Natural Products Chemistry* (1st ed., Vol. 41). Elsevier.

Roland AH van Oorschot, K. N. (2010). Forensic trace DNA: a review. *Investigative Genetics, 1*(14).

Srivastava, L. M. (2002). *Plant Growth and Development : Hormones and Environment.* Elsevier Science & Technology.

T. Doheny-Adams, K. R. (2017). Development of an efficient glucosinolate extraction method. *Plant Methods, 13*(17).

Tetsuya Hama, K. S. (2019). Probing the Molecular Structure and Orientation of the Leaf Surface of Brassica Oleracea L. by Polarization Modulation-Infrared Reflection-Absorption Spectroscopy. *Plant and Cell Physiology, 60*(7), 1567-1580.

W. Steglich, B. F.-F. (Ed.). (2000). *RÖMPP Encyclopedia Natural Products, 1st Edition, 2000* (1st ed.). Thieme.